

1. Report No. SWUTC/05/167827-1	2. Government Accession No.	3. Recipient's Catalog No.	
4. Title and Subtitle Methodology for Quantifying Pavement Damage Caused by Different Axle and Load Configurations		5. Report Date April 2005	
		6. Performing Organization Code	
7. Author(s) Karan Kapoor and Jorge A. Prozzi		8. Performing Organization Report No. Report 167827-1	
9. Performing Organization Name and Address Center for Transportation Research University of Texas at Austin 3208 Red River, Suite 200 Austin, Texas 78705-2650		10. Work Unit No. (TRAIS)	
		11. Contract or Grant No. 10727	
12. Sponsoring Agency Name and Address Southwest Region University Transportation Center Texas Transportation Institute Texas A&M University System College Station, Texas 77843-3135		13. Type of Report and Period Covered	
		14. Sponsoring Agency Code	
15. Supplementary Notes Supported by general revenues from the State of Texas.			
16. Abstract In the past, pavement design has been based on empirical approach, which is accurate if used within the range of design factors over which the methods were developed. However, in an environment of constantly changing designs, materials, traffic characteristics, and construction techniques, there is a continuous need for a design approach which can account for these changing scenarios and increased weight limits. The mechanistic-based analysis approach developed through research project NCHRP 1-37A (Development of the 2002 Guide for the Design of New and Rehabilitated Pavement Structures) explains the scientific basis for pavement deterioration and is used for this research. As part of this research, a number of pavement structures were modeled, different axle load levels were applied, and the response and performance of the pavement sections were estimated under five typical environmental conditions, which fully represent the state of Texas. This report presents and discusses the results of the mechanistic-based performance analysis and the use of the results together with statistical tools to develop a methodology for estimating load-associated pavement damage. The methodology also enables Equivalent Damage Factors (EDF) to be determined for similar pavement structures and environmental conditions.			
17. Key Words Pavement Design, Mechanistic-Empirical, Equivalent Damage Factor (EDF)		18. Distribution Statement No restrictions. This document is available to the public through NTIS: National Technical Information Service 5285 Port Royal Road Springfield, Virginia 22161	
19. Security Classif.(of this report) Unclassified	20. Security Classif.(of this page) Unclassified	21. No. of Pages 108	22. Price

Methodology for Quantifying Pavement Damage Caused by Different Axle and Load Configurations

By
Karan Kapoor
and
Jorge A. Prozzi

Research Report SWUTC/05/167827-1

Southwest Region University Transportation Center

Center for Transportation Research

University of Texas at Austin

Austin, Texas 78712

April 2005

DISCLAIMER

The contents of this report reflect the views of the authors, who are responsible for the facts and the accuracy of the information presented herein. This document is disseminated under the sponsorship of the Department of Transportation, University Transportation Centers Program, in the interest of information exchange. Mention of trade names or commercial products does not constitute endorsement or recommendation for use.

ACKNOWLEDGEMENTS

The authors recognize that support for this research was provided by a grant from the U.S. Department of Transportation, University Transportation Centers Program to the Southwest Region University Transportation Center which is funded 50 percent with general revenue funds from the State of Texas.

ABSTRACT

In the past, pavement design has been based on empirical approach, which is accurate if used within the range of design factors over which the methods were developed. However, in an environment of constantly changing designs, materials, traffic characteristics, and construction techniques, there is a continuous need for a design approach which can account for these changing scenarios and increased weight limits. The mechanistic-based analysis approach developed through research project NCHRP 1-37A (Development of the 2002 Guide for the Design of New and Rehabilitated Pavement Structures) explains the scientific basis for pavement deterioration and is used for this research. As part of this research, a number of pavement structures were modeled, different axle load levels were applied, and the response and performance of the pavement sections were estimated under five typical environmental conditions, which fully represent that which occurs throughout Texas. This report presents and discusses the results of the mechanistic-based performance analysis and the use of the results together with statistical tools to develop a methodology for estimating load-associated pavement damage. The methodology also enables Equivalent Damage Factors (EDF) to be determined for similar pavement structures and environmental conditions.

EXECUTIVE SUMMARY

Introduction and Motivation

In the past, pavement design has been based on empirical approach, which is based on the results of experiments or experience. However, in recent years, there has been an increase in the maximum allowable gross vehicle weights and axle loads. This increase in the allowable gross vehicle weight causes a more-than-proportional increase in the deterioration of pavement conditions (Luskin and Walton 2001), and has necessitated the need for developing improved pavement design and analysis methods.

Empirical models are accurate if used within the range of design factors over which the methods were developed. However, in an environment of constantly changing designs, materials, traffic, and construction characteristics, there is a continuous need for experimentation to keep the empirical methods current. This involves significant costs and it is for this and other such compelling reasons that there has been a major thrust to develop a scientific explanation of the interaction between the pavement structure and materials and the environmental conditions and axle loadings (ERES 2002).

In recent years, the theoretical approach has proven to be useful in explaining the experimental observations (Croney and Croney 1997). In addition, several mechanistic-based design procedures, which make use of mechanistic models such as multi layered elastic model, finite elements model, dynamic model, and viscoelastic model (WSDOT 1998) have been developed and implemented. The success of such development has increased the interest in expanding the scope of theoretical research beyond the validation and verification stage to a more comprehensive design procedure (ERES 2002). The mechanistic-empirical approach symbolizes the paradigm shift in pavement design.

Objectives

This research is aimed at developing a methodology for quantifying the damage caused to flexible pavement structures by various axle and load configurations in varying climatic

conditions using the mechanistic-empirical approach. The major objectives of this research include:

1. evaluation of the mechanistic-empirical design approach for the design and analysis of flexible pavements,
2. evaluation of the impact of traffic volume on different pavement structures and analyzing the surface rutting and fatigue cracking of the structures at various locations in Texas,
3. assessment of the impact of varied axle loads and configurations (single and tandem axles) on rutting and fatigue cracking in different pavement structures at various locations in Texas, and
4. evaluation of the relative pavement life based on a standard load configuration, using Equivalent Damage Factors (EDF).

Flexible Pavements

Flexible pavements typically consist of a multi-layer structure. There are three types of flexible pavements (Huang 2004):

1. conventional flexible pavements — are layered systems with better materials on top and inferior materials at the bottom,
2. full-depth asphalt pavements — one or more layers of hot mix asphalt (HMA) immediately over the subgrade, and
3. contained rock asphalt mats — four layers that are laid over a conventionally prepared subgrade.

For the purpose of this research study, conventional flexible pavements composed of four layers — asphalt surface, untreated granular base and subbase courses, and natural subgrade — are selected. The asphalt surface is the top course of a flexible pavement, usually constructed of dense graded HMA. The layers below the asphalt surface are the base and subbase courses, which are composed of untreated granular materials. This three-layer system rests on top of the natural soil, or subgrade, which for modeling purposes is considered to be a semi-infinite medium (Huang 2004).

Since World War II, pavement design has largely been derived through the results of full-scale experiments and detailed study of the performance of in-service pavements (ERES 2002). There has been increasing research in the development of more fundamental structural procedures which are aimed at relating the stresses and strains produced by traffic loading in pavement materials with the performance of those materials under repetitive loading. Full-scale experiments conducted with a range of different traffic conditions, environments, construction materials, axle configurations, and different layer conditions are expensive and time consuming. Analytical models can be combined with the empirical approach in order to understand the way flexible pavements perform under different traffic conditions, axle configurations, and weights (ERES 2002).

In mechanistic-empirical analyses, pavement responses such as stresses, strains, and deflections are evaluated in various points of a pavement cross-section using mechanistic modeling tools such as finite element models and elastic layer analysis. The pavement performance is then evaluated using empirical models in terms of various mechanisms such as rutting, fatigue cracking, and thermal cracking. Technically, a mechanistic-empirical approach to pavement design is the most sophisticated way of modeling pavements (ERES 2002).

Need for the Mechanistic-Empirical Design Approach

There are several reasons why the traditional approach of empirical pavement design should be revised to the mechanistic-empirical approach. For instance, the empirical approach is based on the results of experiments, so when a pavement is to be designed outside the conditions that are used for these experiments, it is not possible to obtain accurate performance estimates. There has been continual improvement in the pavement industry over the years with the development of new construction materials, construction methods, vehicle suspension systems, and tires. For these reasons the performance of existing pavements provides little guidance as to how pavements built with new materials and methods will perform (ERES 2002). In addition to the increase in axle loads, the nation's highways are also carrying new trucks with different axle and load configurations. The empirical models can only suggest how pavements would respond to

these new axle and load configurations. Thus it is extremely difficult to predict pavement performance for future needs based on past practices (ERES 2002).

A large number of design features have a significant impact on pavement design and are not considered in the empirical approach. For the design of asphalt concrete (AC) pavement, conventional procedures do not take into consideration the ordering of the different structural layers, nor do they have a means of incorporating non-conventional materials in design. These issues can be addressed in the mechanistic-empirical approach (ERES 2002).

Methodology

For the purpose of this research study, six pavement structures were analyzed. In order to analyze the performance of the pavement structures under varied climatic conditions, five different locations were selected in Texas: Austin, Amarillo, Dallas/Fort Worth, El Paso and Houston Intercontinental Airport.

The rationale behind the selection of the locations was to represent different geographical locations and varying climatic conditions existing in Texas.

After the experimental locations were chosen, the six pavement structures were designed, design ESAL values were calculated, and daily traffic was estimated for the various structures in order for the pavements to reach failure in terms of rutting and fatigue cracking at the end of the performance period. The failure criteria were chosen as 0.5 inches of rutting and 10 percent fatigue cracking. A performance period of 20 years was used for the analysis.

“Empirical AADTT” values were obtained based on the AASHTO 1993 Design Guide. Using these empirical values, the structures were analyzed for failure in terms of rutting and fatigue cracking performance. It was observed that pavement deterioration was slowest in Amarillo as compared to the other four locations. Hence it was decided to use Amarillo as the test location, and the smallest axle load of 12 kips single axle was used to determine the “mechanistic AADTT

values” for the six structures. It should be noted that these “mechanistic-based AADTT” values are expressed in single axles rather than actual trucks.

The traffic volume needed to reach failure was compared with the empirical traffic volumes. If the failure was not obtained as predicted, the AADTT values were adjusted to reach failure as predicted. Reviewing the results it was observed that for a given AADTT value, even though a pavement reached 0.5-inch rutting, fatigue cracking was well below 10 percent. The results necessitated the need to use different AADTT values for the analysis of pavement failure in terms of rutting and fatigue cracking for a given structure.

In the last part of this research study, pavement life is evaluated relative to the life under the standard 18-kips single axle load. Since load repetitions indicate the pavement life for different axle loads, the pavement life varies under different axle loads making it difficult to determine generalized trends.

Conclusions

The recently developed mechanistic-empirical-based Design Guide was used in this research for the evaluation of pavement performance and the determination of EDF. The four major variables that were considered in this research study are:

1. pavement structural capacity (expressed in terms of the structural number (SN)),
2. environmental conditions (five locations representative of the most typical Texas conditions were investigated),
3. axle loads (single and tandem axles), and
4. rutting and fatigue-cracking performance.

The failure criterion of the pavements in terms of surface rutting was 0.5 inches and 10 percent in terms of fatigue cracking. When compared to the empirical design based on American Association of State Highway and Transportation Officials (AASHTO) 1993, the mechanistic-based analysis estimates longer pavement lives for structures 1 and 2 and a similar estimate for structure 3. On the other hand, for structures 4, 5 and 6, the mechanistic-based analysis estimates

longer pavement lives in terms of fatigue, and shorter pavement lives in terms of rutting compared to the empirical-based analysis. However, the failure criterion in AASHTO 1993 is based on riding quality in terms of Present Serviceability Index (PSI). Expected life as a function of the SN is sensitive when applying the empirical method, but markedly less sensitive when the mechanistic approach is used.

Based on the performance analyses, it was observed that Amarillo had the slowest pavement deterioration compared to the other locations that were chosen for this research project. This pace of deterioration was attributed to the colder weather that prevails in Amarillo. On the other hand, the fastest pavement deterioration was observed in Austin and El Paso, which could be accredited to their warmer climate.

The effect of using different axle loads for both single and tandem axles was also investigated as part of this research study. It was observed that as the axle load increased, the pavement reached failure at a faster rate, requiring a lower number of repetitions to reach failure. It was also observed that as the axle load increased, the fatigue-based EDF increased at a much faster rate compared to rutting-based EDF. In all instances, the deterioration occurred more slowly in Amarillo than the other locations.

EDF is the analysis of relative pavement life based on a standard axle load. The standard axle load chosen was 18,000 lbs. for single axle loads and 34,000 lbs. for tandem axle loads.

Regression analysis enabled the formulation of simple equations for estimating EDF directly. Variables such as axle loads, SN, and locations were considered, but only axle loads had a statistically significant impact on the EDF. From these equations, it was concluded that fatigue-based EDF increased at a faster rate compared to rutting-based EDF when the axle load increased. This result was due to the fact that the SN term had a positive fatigue slope and a negative rutting slope.

Another observation was that as the SN increased to a particular value, which is the critical value of the SN, fatigue life decreased. As the SN was further increased, fatigue life increased. This critical value of the SN was observed to be between 3 and 4.

In order to see the application of these equations and to be able to compare the results of the estimated EDF values with those obtained by using the Design Guide, a case study was conducted. The error between the estimated and the actual values was low for both fatigue and rutting, hence representing reliable equations for EDF formulation. The impact of overloading was also evaluated, which showed that the increase in pavement deterioration is more than proportional to the increase in axle loads.

TABLE OF CONTENTS

CHAPTER 1. INTRODUCTION	1
1.1 Introduction and Motivation	1
1.2 Objectives	1
1.3 Flexible Pavements	2
1.4 Need for the Mechanistic-Empirical Design Approach	3
1.5 Report Outline	4
CHAPTER 2. BACKGROUND	5
2.1 Flexible Pavement Structures	5
2.2 Pavement Responses	7
2.3 Material Characterization	8
2.4 Pavement Design Approaches	9
2.5 Empirical Approach	10
2.6 Mechanistic Approach	11
2.7 Mechanistic-Empirical Approach	11
2.8 Benefits of the Mechanistic-Empirical Approach	14
2.9 NCHRP 1-37A Project Methodology	14
2.10 Design Inputs	15
2.11 Number of Repetitions	16
2.12 Failure Mechanisms	16
2.13 Road Traffic and Axle Loading	20
CHAPTER 3. EXPERIMENTAL SET-UP AND METHODOLOGY	25
3.1 Experimental Set-up	25
3.2 Methodology	31
CHAPTER 4. RESULTS AND ANALYSIS	33
4.1 Results	33
4.2 Equivalent Damage Factors (EDF)	54
CHAPTER 5. REGRESSION ANALYSIS AND APPLICATIONS	69
5.1 Regression Analysis	69

5.2	Case Study.....	74
CHAPTER 6. CONCLUSIONS AND RECOMMENDATIONS.....		77
6.1	Conclusions.....	77
6.2	Future Research.....	79
REFERENCES.....		81
APPENDIX A. BETA VERSION OF THE 2002 DESIGN GUIDE.....		85

LIST OF ILLUSTRATIONS

Figures

Figure 2.1.	Four-Layered Pavement Structure.....	7
Figure 2.2.	Mechanistic-Empirical Methodology.....	13
Figure 2.3.	Texas Vehicle Classification.....	22
Figure 2.4.	FHWA Vehicle Classification.....	23
Figure 3.1.	Experimental Locations.....	26
Figure 3.2.	Gradation Curve for Different Materials.....	28
Figure 4.1.	Rutting Life for 18 kips Standard Single Axle Load.....	35
Figure 4.2.	Rutting Life of Structure 1 for Single Axle Loads.....	36
Figure 4.3.	Rutting Life of Structure 2 for Single Axle Loads.....	37
Figure 4.4.	Rutting Life of Structure 3 for Single Axle Loads.....	37
Figure 4.5.	Rutting Life of Structure 4 for Single Axle Loads.....	38
Figure 4.6.	Rutting Life of Structure 5 for Single Axle Loads.....	38
Figure 4.7.	Rutting Life of Structure 6 for Single Axle Loads.....	39
Figure 4.8.	Rutting Life of Structure 1 for Tandem Axle Loads.....	41
Figure. 4.9.	Rutting Life of Structure 2 for Tandem Axle Loads.....	42
Figure 4.10.	Rutting Life of Structure 3 for Tandem Axle Loads.....	42
Figure 4.11.	Rutting Life of Structure 4 for Tandem Axle Loads.....	43
Figure 4.12.	Rutting Life of Structure 5 for Tandem Axle Loads.....	43
Figure 4.13.	Rutting Life of Structure 6 for Tandem Axle Loads.....	44
Figure 4.14.	Fatigue Life for 18 kips Standard Single Axle Load.....	46
Figure 4.15.	Fatigue Life of Structure 1 for Single Axle Loads.....	47

Figure 4.16.	Fatigue Life of Structure 2 for Single Axle Loads	47
Figure 4.17.	Fatigue Life of Structure 3 for Single Axle Loads	48
Figure 4.18.	Fatigue Life of Structure 4 for Single Axle Loads	48
Figure 4.19.	Fatigue Life of Structure 5 for Single Axle Loads	49
Figure 4.20.	Fatigue Life of Structure 6 for Single Axle Loads	49
Figure 4.21.	Fatigue Life of Structure 1 for Tandem Axle Loads	51
Figure 4.22.	Fatigue Life of Structure 2 for Tandem Axle Loads	52
Figure 4.23.	Fatigue Life of Structure 3 for Tandem Axle Loads	52
Figure 4.24.	Fatigue Life of Structure 4 for Tandem Axle Loads	53
Figure 4.25.	Fatigue Life of Structure 5 for Tandem Axle Loads	53
Figure 4.26.	Fatigue Life of Structure 6 for Tandem Axle Loads	54
Figure 4.27(a).	EDF Values Using 18 kips Single Axle as the Standard Load for Pavements to Reach 0.5-inch Rutting	58
Figure 4.27(b).	EDF Values Using 18 kips Single Axle as the Standard Load for Pavements to Reach 0.5-inch Rutting	59
Figure 4.28(a).	EDF Values Using 34 kips Tandem Axle as the Standard Load for Pavements to Reach 0.5-inch Rutting	60
Figure 4.28(b).	EDF Values Using 34 kips Tandem Axle as the Standard Load for Pavements to Reach 0.5-inch Rutting	61
Figure 4.29(a).	EDF Values Using 18 kips Single Axle as the Standard Load for Fatigue Cracking	65
Figure 4.29(b).	EDF Values Using 18 kips Single Axle as the Standard Load for Fatigue Cracking	66
Figure 4.30(a).	EDF Values Using 34 kips Tandem Axle as the Standard Load for Fatigue Cracking	67
Figure 4.30(b).	EDF Values Using 34 kips Tandem Axle as the Standard Load for Fatigue Cracking	68
Figure 5.1.	Axle Loads (kips) for a Class 9 Vehicle Used in the Case Study	74
Figure A.1.	Input Screen of 2002 Design Guide	86
Figure A.2.	General Information Inputs	87

Figure A.3.	Pavement Layers.....	88
Figure A.4.	Locations.....	88
Tables		
Table 3.1.	Test Locations.....	25
Table 3.2.	Pavement Layers.....	29
Table 3.3.	Layer Thicknesses.....	29
Table 3.4.	Empirical Traffic Volumes.....	30
Table 3.5.	Axle Loads Used in this Research.....	31
Table 3.6.	AADTT Values for the Pavements to Reach Failure in Terms of Rutting and Fatigue Cracking.....	32
Table 4.1.	Empirical and Mechanistic-Empirical Design Lives.....	33
Table 4.2.	Rutting Life for Single Axle Loads.....	34
Table 4.3.	Rutting Life for Tandem Axle Loads.....	40
Table 4.4.	Fatigue Life for Single Axle Loads.....	45
Table 4.5.	Fatigue Life for Tandem Axle Loads.....	50
Table 4.6.	EDF Values Using 18 kips Single Axle as the Standard Load for Pavements to Reach 0.5-inch Rutting.....	56
Table 4.7.	EDF Values Using 34 kips Tandem Axle as the Standard Load for Pavements to Reach 0.5-inch Rutting.....	57
Table 4.8.	EDF Under Varying Axle Loads–10 Percent Fatigue Cracking.....	63
Table 4.9.	EDF Under Varying Axle Loads–10 Percent Fatigue Cracking.....	64
Table 5.1.	Regression Models for Fatigue-based EDF.....	70
Table 5.2.	Regression Models for Rutting-based EDF.....	72
Table 5.3.	Final Regression Models for Fatigue- and Rutting-based EDF.....	73
Table 5.4.	Structural Properties of the Sample Structure.....	74
Table 5.5.	Estimated EDF Values for Austin.....	75

Table 5.6.	Estimated EDF Values for Dallas.....	75
Table 5.7.	Estimated EDF Values for Waco.....	75
Table 5.8.	Estimated vs. Actual Fatigue and Rutting Lives for Waco.....	76

Chapter 1. Introduction

1.1 Introduction and Motivation

For the past, pavement design has been based on the empirical approach, which is based on the results of experiments or experience (discussed in Section 2.3). However, in recent years, there has been an increase in the maximum allowable gross vehicle weights and axle loads. This increase in the allowable gross vehicle weight causes a more-than-proportional increase in the deterioration of pavement conditions (Luskin and Walton 2001), and has necessitated the need for developing improved pavement design and analysis methods.

Empirical models are accurate if used within the range of design factors over which the methods were developed. However, in an environment of constantly changing designs, materials, traffic, and construction characteristics, there is a continuous need for experimentation to keep the empirical methods current. This involves significant cost, and it is for this and other such compelling reasons that there has been a major thrust to develop a scientific explanation of the interaction between pavement structure and materials and the environmental conditions and axle loadings (ERES 2002).

In recent years, the theoretical approach has proven to be useful in explaining the experimental observations (Croney and Croney 1997). In addition, several mechanistic-based design procedures, which make use of mechanistic models such as multi-layered elastic, finite elements, dynamic, and viscoelastic (WSDOT 1998), have been developed and implemented. The success of such development has increased the interest in expanding the scope of theoretical research beyond the validation and verification stage to a more comprehensive design procedure (ERES 2002). The mechanistic-empirical approach symbolizes the paradigm shift in pavement design.

1.2 Objectives

This research is aimed at developing a methodology for quantifying the damage caused to flexible pavement structures by various axle and load configurations in varying climatic

conditions using the mechanistic-empirical approach. The major objectives of this research include:

1. evaluation of the mechanistic-empirical design approach for the design and analysis of flexible pavements,
2. evaluation of the impact of traffic volume on different pavement structures and analyzing the surface rutting and fatigue cracking of the structures at various locations in Texas,
3. assessment of the impact of varied axle loads and configurations (single and tandem axles) on rutting and fatigue cracking in different pavement structures at various locations in Texas, and
4. evaluation of the relative pavement life based on a standard load configuration, using Equivalent Damage Factors (EDF).

1.3 Flexible Pavements

Flexible pavements typically consist of a multi-layer structure. There are three types of flexible pavements (Huang 2004):

1. conventional flexible pavements — layered systems with better materials on top and inferior materials at the bottom (explained in Section 2.1.1),
2. full-depth asphalt pavements — one or more layers of hot mix asphalt (HMA) immediately over the subgrade (discussed in Section 2.1.2), and
3. contained rock asphalt mats — four layers that are laid over a conventionally prepared subgrade (discussed in Section 2.1.3).

For the purpose of this study, conventional flexible pavements composed of four layers (asphalt surface, untreated granular base and subbase courses, and natural subgrade) are selected. The asphalt surface is the top course of a flexible pavement, usually constructed of dense graded hot HMA. The layers below the asphalt surface are the base and subbase courses, which are composed of untreated granular materials. This three-layer system rests on top of the natural soil, or subgrade, which for modeling purposes is considered to be a semi-infinite medium (Huang 2004).

Since World War II, pavement design has largely been derived through the results of full-scale experiments and detailed study of the performance of in-service pavements (ERES 2002). There has been increasing research in the development of more fundamental structural procedures which are aimed at relating the stresses and strains produced by traffic loading in pavement materials with the performance of those materials under repetitive loading. Full-scale experiments conducted with a range of different traffic conditions, environments, construction materials, axle configurations, and different layer conditions are expensive and time consuming. Analytical models can be combined with the empirical approach in order to understand the way flexible pavements perform under different traffic conditions, axle configurations, and weights (ERES 2002).

In mechanistic-empirical analyses, pavement responses such as stresses, strains, and deflections are evaluated in various points of a pavement cross-section using mechanistic modeling tools such as finite element models and elastic layer analysis. The pavement performance is then evaluated using empirical models in terms of various mechanisms such as rutting, fatigue cracking, and thermal cracking. Technically, a mechanistic-empirical approach to pavement design is the most sophisticated way of modeling pavements (ERES 2002).

1.4 Need for the Mechanistic-Empirical Design Approach

There are several reasons why the traditional approach of empirical pavement design should be revised to the mechanistic-empirical approach. For instance, the empirical approach is based on the results of experiments, so when a pavement is to be designed outside the conditions that are used for these experiments, it is not possible to obtain accurate performance estimates. There has been continual improvement in the pavement industry over the years with the development of new construction materials, construction methods, vehicle suspension systems, and tires. For these reasons the performance of existing pavements provides little guidance as to how pavements built with new materials and methods will perform (ERES 2002). In addition to the increase in axle loads, the nation's highways are also carrying new trucks with different axle and load configurations. The empirical models can only suggest how pavements will respond to these

new axle and load configurations. Thus it is extremely difficult to predict pavement performance for future needs based on past practices (ERES 2002).

A large number of design features have a significant impact on pavement design and are not considered in the empirical approach. For the design of asphalt concrete (AC) pavement, conventional procedures do not take into consideration the ordering of the different structural layers, nor do they have means of incorporating non-conventional materials in design. These issues can be addressed in the mechanistic-empirical approach (ERES 2002).

1.5 Report Outline

An overview of flexible pavement structures, pavement design approaches, and mechanistic-empirical approach is presented in Chapter 2, along with the design inputs and distress models used in this methodology. Pavement failure mechanisms, along with road traffic, axle loading, types of vehicles, and material characterization are also described in this chapter.

Chapter 3 describes the experimental set-up, which includes environmental conditions, pavement structures, material properties, traffic volume, pavement structural capacity, and axle loads. The methodology used for this research study, including the design inputs and Average Annual Daily Truck Traffic (AADTT) values is also explained in this chapter.

Results of the performance analyses at various locations for all the structures are discussed in Chapter 4. The number of axle repetitions for the pavements to reach failure in terms of surface rutting and fatigue cracking are discussed in this chapter. Chapter 4 also includes EDF analysis for rutting and fatigue cracking using single and tandem axles.

Regression analysis along with a case study for a sample structure is given in Chapter 5. Finally, the conclusions and recommendations are given in Chapter 6.

CHAPTER 2. BACKGROUND

2.1 Flexible Pavement Structures

Flexible pavements are layered systems constructed of bituminous and granular materials. The upper layer is the asphalt layer, which is usually constructed of dense graded HMA. The lower layers are composed of different combinations of granular materials. Three types of flexible pavements (Huang 2004) are described in the following sections.

2.1.1 Conventional Flexible Pavements

Conventional flexible pavements are layered systems that consist of stronger and better quality materials on top, as the intensity of the stresses is high on top and inferior quality materials at the bottom. Typically this type of pavement consists of the following layers from top to bottom:

1. Seal coat is the thin asphalt surface treatment used for waterproofing the surface or providing skid resistance to the surface.
2. Surface Course is the top course of an asphalt pavement and is usually constructed with HMA.
3. Binder course is the asphalt base course typically consisting of coarser aggregates and less asphalt compared to the surface course. The reason for using a binder course in addition to the surface course is that HMA could be too thick to be compacted in one layer.
4. Tack coat is a very thin application of asphalt uniformly covering the entire surface to be paved, and is used to ensure a bond between the surface being paved and the overlying course.
5. Prime coat has the function of binding the granular base to the asphalt layer in the form of an application of low-viscosity cutback asphalt, which is asphalt cement that has been blended with a diluent of petroleum solvents (DRDB 1997).
6. Base course is the layer of material directly below the binder course, which may be comprised of crushed stone, crushed slag, or other stabilized materials.

7. Subbase course is the layer below the base course. The use of two different granular materials is to reduce cost. Instead of using more expensive material for the entire layer, costs can be reduced by using less expensive materials for the subbase course above the subgrade course.
8. Subgrade is the last layer, underneath the subbase course. The top 6 inches of the subgrade are scarified and compacted to the desirable density. This compacted subgrade can be the in-situ soil or a layer of a particular material.

2.1.2 Full Depth Asphalt Pavements

Full depth asphalt pavement consists of one or more layers of HMA immediately over the subgrade. The concept was introduced by the Asphalt Institute and is supposed to be the most dependable form of asphalt pavement for heavy traffic (Asphalt Institute 1987). This type of pavement is effective in locations where local materials are not readily available and so eliminates the need to purchase several types of materials.

2.1.3 Contained Rock Asphalt Mats

A contained rock asphalt mat is a four-layer structure with the bottommost layer consisting of modified dense graded HMA spread over a conventionally prepared subgrade. The next layer is open graded aggregate, followed by a layer of dense graded aggregate. The top layer is composed of dense graded HMA.

For the purpose of this research, six pavement structures were analyzed, each being conventional flexible pavements of four layers (Fig 2.1). Each structure is composed of different layer thicknesses made of the same material.

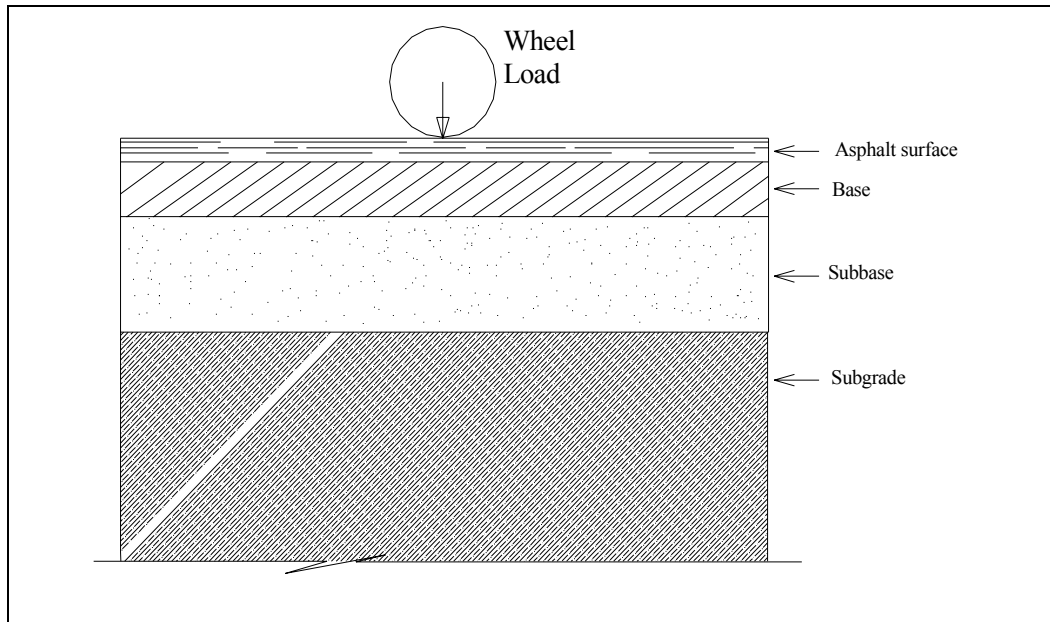


Figure 2.1: Four-Layered Pavement Structure

2.2 Pavement Responses

The pavement responses that are calculated using mechanistic models such as multi-layered linear elastic and finite elements models are stresses, strains, and deflections. Critical pavement responses are estimated from the structural response models based on the loadings applied, pavement layer thicknesses, and material properties. For the purpose of this research, a multi-layer linear-elastic structural model was used. Hence, each layer can be uniquely characterized by its elastic modulus, Poisson's ratio and thickness.

A wheel load produces stresses and strains in the pavement structure that are transmitted from the top to the bottom layers. These stresses reduce as the depth increases. Reduction of stress depends on modulus and thickness of the layer. One of the major functions of pavement is to reduce stresses transmitted to the subgrade to such an extent that the soil will withstand the stresses without excessive deformation. For this reason, the structural design of pavement must be equated with the axle loads the pavement will carry and the strength and deformation characteristics of the subgrade (ERES 2002).

A wheel load applied to the pavement surface causes deflection in the pavement. The magnitude of this deflection under the wheel load is proportional to the overall stiffness of the pavement, modulus of the subgrade, and stiffness of the individual layers (ERES 2002).

Modeling of loads for multi-layered linear elastic systems assume that the loads are static, have uniform contact pressures, and that the contact areas of the tires are circular (ERES 2002). While these are important limitations of the multi-layered linear elastic model, the practical advantages of these assumptions surpass the limitations. The practical advantages include the ability to fully characterize a material with three properties, and the computational simplicity and speed of estimating pavement responses.

2.3 Material Characterization

For the purpose of this research study, response properties and distress properties were considered. Response properties, such as the elastic modulus and Poisson's ratio, are needed in order to predict the states of stress, strain and displacement within the structure. On the other hand, distress properties are used through transfer functions in order to predict the major modes of distress associated with a particular material such as fatigue and permanent deformation (rutting) of asphalt pavements (Croney and Croney 1997).

The structural behavior of bituminous materials in road pavements is complex in nature. Some of the permanent deformation that occurs in a pavement is within the bituminous materials, most of which are not elastic and experience some permanent deformation after each load application. Still, if the load is repeated a number of times and is small in comparison to the load-bearing capacity of the pavement, the deformation under each load is almost completely recoverable and is proportional to the load, and hence can be considered elastic (Huang 2004).

The stiffness properties of bituminous materials are known to be a function of temperature, loading rate, age and mixture characteristics such as binder stiffness, aggregate gradation, binder content, and air voids (Monismith 1992).

Resilient modulus is the ratio of the applied stress to the elastic strain and relates to the elastic component of the response only. It is usually based on stress and strain measurements from rapidly applied loads similar to those that pavement materials experience from wheel loads. At temperatures higher than 77°F (25°C) it is possible that the stress state has an influence on the stiffness characteristics of these materials (Monismith 1992). The dynamic modulus of a material is a viscoelastic test response developed under sinusoidal loading conditions. It is the absolute value of dividing the peak-to-peak stress by the peak-to-peak strain for a material subjected to a sinusoidal loading, which varies with the loading frequency (Harman 2001). Differences in dynamic modulus are usually insignificant among tension, tension-compression and compression tests for temperatures ranging from 40° to 70°F (4 to 21°C) (Huang 2004). The current version of the Design Guide 2002 uses dynamic modulus for characterization of the mixes for the design of pavement structures.

In the case of granular materials, there is substantial deformation with the application of the initial load. But as the number of load repetitions increases, there is little increase in surface deformation (Huang 2004).

The primary factors affecting stiffness characteristics of granular materials are water content and dry density. Stiffness properties of granular materials are dependent on the applied stresses (Monismith 1992). The elastic modulus, used for the analysis of layer systems composed of granular materials under moving loads, is the resilient modulus. The resilient modulus of granular materials can be determined from repeated load triaxial compression tests (Huang 2004).

2.4 Pavement Design Approaches

In order to design a pavement structure, guidelines related to traffic loads, traffic volumes, material types, environmental conditions, drainage, and pavement thickness must be established. Such design specifications can either be developed based on in-situ testing of pavements — which is the principle of empirical methodology explained in Section 2.5 — or by the

mechanistic approach as explained in Section 2.6. Another approach for designing pavements is the mechanistic-empirical methodology, which is discussed in Section 2.7.

Pavement performance models can also be used in the pavement design and analysis process. A pavement performance model is an equation which relates variables such as pavement layer thickness, material strength, climatic conditions, applied load, and wheel and axle configurations to performance indicators. The models are developed by correlating theoretical relationships between structural responses and distresses with observed distresses in the field, from performance data of a large number of pavements. Some of the distresses for flexible pavements, for which performance equations exist, are rutting, fatigue cracking, thermal cracking, and smoothness (ERES 2002).

2.5 Empirical Approach

An empirical approach is based on the results of experiments and involves building pavement test sections representing a wide range of road materials and subjecting them to actual or simulated traffic loads. Empirical models are used in this approach. There are three different approaches to conducting these experiments:

1. Long Term Pavement Performance (LTPP), wherein, experiments are carried out over a period of several years on pavements that are subject to normal traffic load (Croney and Croney 1997).
2. Accelerated pavement testing (APT), which was used in the Western Association of State Highway Organizations (WASHO) Road Test in Idaho during 1953-54 and in the American Association of State Highway Officials (AASHO) Road Test in Illinois during 1958-1960. APT can be performed using mobile machines, fixed machines or test trucks (ERES 2002). Although this approach produces results more quickly than LTPP, it should be noted that aging of the pavement materials is not taken into account due to the accelerated traffic that is used in a relatively short period of time (Croney and Croney 1997).
3. Laboratory testing approach, wherein tests are conducted for evaluating pavement materials under laboratory settings (Croney and Croney 1997). These laboratory testing

methods provide information regarding the properties of the pavement system materials and data needed to evaluate existing specifications and design methods. Shift factors, which are the statistical correlations, are used to relate various laboratory testing methods with in-situ methods and APT methods.

2.6 Mechanistic Approach

A mechanistic approach provides a scientific basis for relating the mechanics of structural behavior to loading. In order to quantify how the load on a structure is distributed to its members, certain basic materials properties must be determined, along with the geometric properties of the structure. Boussinesq (1885) was the first to apply a mechanistic approach to the two-layered systems, followed by Burmister who, during the 1940's, developed elastic-layered theory to compute stresses, strains, and deflections in flexible pavements. In the mechanistic approach, mechanistic models are used to generate pavement responses in terms of stresses, strains and deflections. To-date, however, there are no mechanistic models for performance prediction. In reality, mechanistic design approach has not been used for pavement design because of the complex nature of pavement design. (ERES 2002). Currently, empirical information is still needed in order to relate theory to the actual pavement performance.

2.7 Mechanistic-Empirical Approach

This research study is based on the methodology developed in the National Cooperative Highway Research Program (NCHRP) Project 1-37A entitled, "Development of the 2002 Guide for the Design of New and Rehabilitated Pavement Structures" (discussed in Section 2.9), which uses the mechanistic-empirical approach. Mechanistic-empirical methodology is the combination of mechanistic approach and empirical approach (NCHRP 1-37A). The mechanistic models generate responses including stresses, strains, and deflections at critical locations of a pavement structure. These models may consist of multi-layered elastic model, finite elements model, dynamic model, and viscoelastic model (ERES 2002). Inputs in such models consist of the fundamental mechanical properties of the materials, applied wheel and axle loads, climatic conditions, and pavement structures including the number and thickness of layers.

Pavement responses are then used as inputs in the empirical models to estimate pavement performance. These empirical models are calibrated using the data obtained from laboratory testing and actual field performance. The empirical models are regression equations which are used to obtain a best fit between actual field performance and predicted distresses. The disadvantage of the regression approach is that the models are limited to the conditions under which they are developed because they cannot include all the variables that affect the predicted distress. When the values of the variables are similar to those in the original data set, the regression models work well. However, when the models are applied to a different situation with different factors, the predictions are not accurate and hence the model requires recalibration. Pavement performance, which is obtained from these empirical models, is measured in terms of distresses such as rutting, fatigue cracking, roughness, and thermal cracking in the mechanistic-empirical approach.

A mechanistic-empirical approach is the most sophisticated and universally applicable approach to pavement design. The approach is based on the fact that if the response of the pavement layer materials to given environmental conditions and traffic can be predicted accurately, the performance of the pavement can be modeled without actually building the structure (ERES 2002).

Some of the major components of the mechanistic-empirical approach (ERES 2002) are:

1. design inputs — traffic, environment, structure, soil;
2. mechanistic (structural) models to estimate responses;
3. empirical models to predict the pavement performance;
4. design variability and reliability; and
5. performance criteria by which the pavement performance is judged.

Figure 2.2 shows the mechanistic-empirical model.

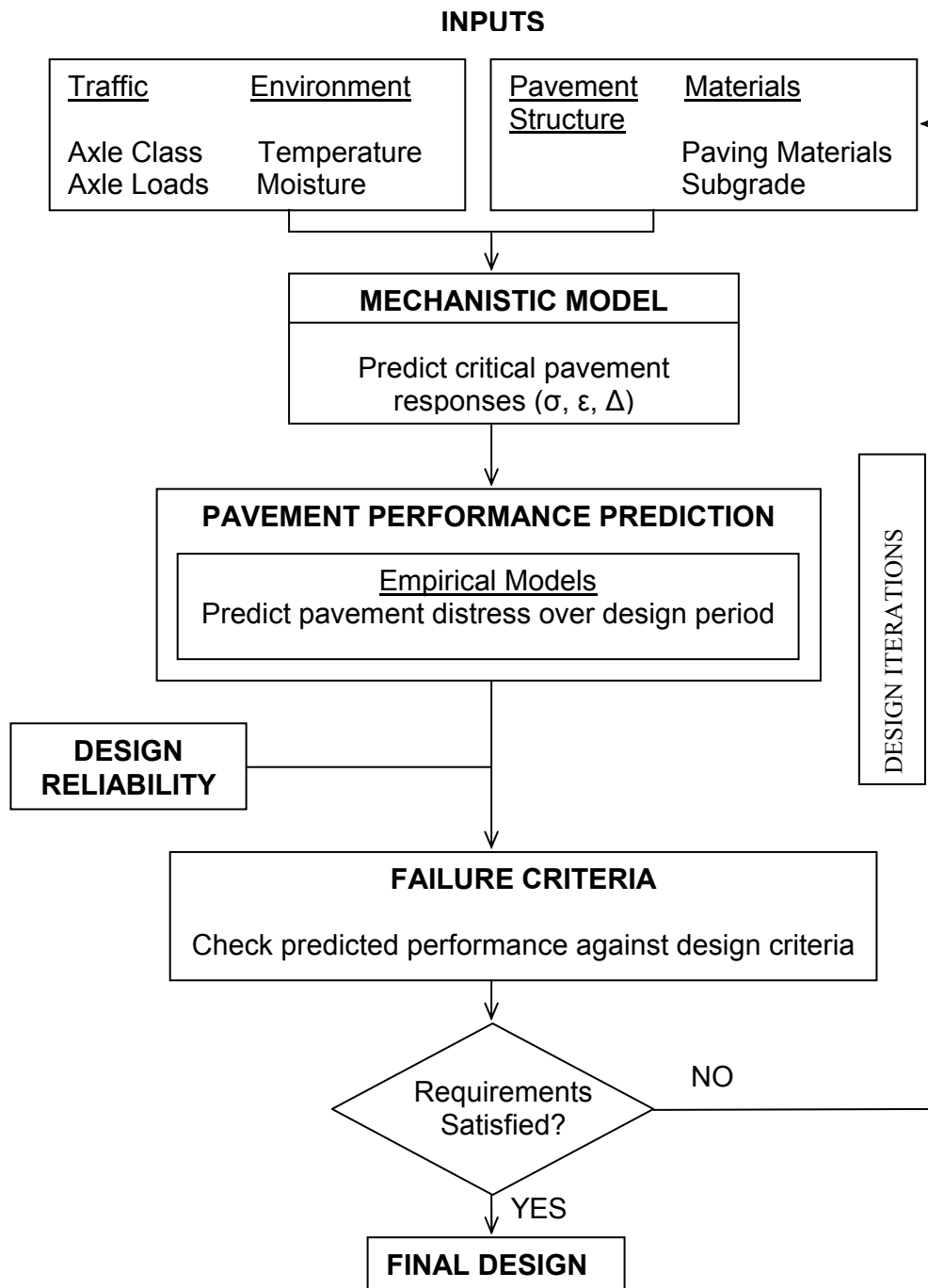


Figure 2.2: Mechanistic-Empirical Methodology (Modified from ERES 2002)

2.8 Benefits of the Mechanistic-Empirical Approach

The mechanistic-empirical design approach developed under NCHRP 1-37A provides the designer with the tools to evaluate the effect of variations in materials on pavement performance, including inherent as well as those due to construction procedures. The mechanistic-empirical approach provides a rational relationship between construction and materials specification and the design of the pavement structure (ERES 2002).

Some additional benefits of the mechanistic-empirical approach (ERES 2002) are:

1. The effects of differences in climatic conditions on pavement performance can be included in the design.
2. Better utilization of the available construction materials can be estimated.
3. Effects of different vehicle types, suspension systems, axle configurations and tire types can be incorporated in the design process.
4. Estimates of the consequences of new loading conditions (like the damaging effects of increased loads) can be evaluated.
5. Better pavement diagnostic techniques, like improved procedures to evaluate premature distress, can be developed.
6. Consideration can be given to seasonal and aging effects on materials and designs.

2.9 NCHRP 1-37A Project Methodology

The objective of NCHRP 1-37A, as the project title implies, was to develop the “2002 Guide for the Design of New and Rehabilitated Pavement Structures” based on engineering mechanics principles. The NCHRP project is based on the mechanistic-empirical methodology for the evaluation of pavement performance (NCHRP 2002).

This new method (hereafter referred to as the Design Guide) is being developed by incorporating a number of years of existing research into a powerful analytical tool for the design and performance analysis of pavement structures. The Design Guide covers new and rehabilitated pavements, including procedures for life-cycle cost analysis and evaluations of the existing

pavements. It is based on a calibrated mechanistic design procedure, which integrates all design variables such as material characterization, environmental conditions, traffic analysis, axle load distributions, and design reliability. For flexible pavements, the structural models include both a multi-layered linear-elastic program and a finite element program for non-linear analysis. The snapshots of some of the input screens used in the current Beta version of the Design Guide software are given in Appendix A.

The Design Guide uses a hierarchical approach for incorporating design input variables according to the importance of the project. There are three levels of inputs which can be selected depending on the requirements of the project. Level 1 is based on site specific measurements and is reserved for the most accurate designs where the consequences of early failure are economically significant. Level 2 is based on regional values or regression equations and is consistent with the current version of the AASHTO Design Guide (AASHTO 1993). Finally, Level 3 design makes use of default values, and hence is the least accurate (ERES 2002). The hierarchical approach applies to all aspects of the design guide including traffic, materials and environmental inputs. Once the inputs have been developed in the design guide, structural (performance) analysis is conducted. This is followed by the evaluation of technically viable alternatives (McGhee 1999).

2.10 Design Inputs

Pavement design inputs vary with the type of structure being designed, and include pavement structure, climatic conditions, pavement materials, soil conditions, and traffic loading. The design inputs can be broadly classified into two categories (ERES 2002):

1. Site variables are those over which the designer has no control and must be accommodated in the design process (e.g., climate, soil conditions, and traffic).
2. Design variables are those over which the designer has control and can change in order to accommodate the design criteria (e.g., the number of pavement layers, type of pavement materials, and layer thicknesses).

2.11 Number of Repetitions

In the Design Guide, pavement performance is expressed as a function of all axle repetitions. For pavement analysis, the pavement performance is expressed in terms of distresses such as surface rutting, top-down fatigue cracking or longitudinal cracking, bottom-up fatigue cracking or alligator cracking, thermal cracking, and fatigue fracture in a chemically stabilized base layer. The number of axle repetitions in the traffic stream necessary to reach pre-established levels of the failure criteria is obtained. For the purpose of this research, these criteria are 0.5 inch of surface rutting and 10 percent fatigue cracking. The number of axle load repetitions to reach the failure criteria is referred to as pavement life.

Another widely accepted pavement analysis procedure is to develop equivalent factors and convert each load group into an equivalent number of 18 kip (80 kN) single axle loads (Section 3.1.4). It is important to note here that the equivalency between two different loads depends on the failure criterion used. Equivalent factors based on rutting may be different from those based on fatigue cracking (Huang 2004). Most of the previous research studies express performance based on the number of Equivalent Single Axle Loads (ESALs) to failure. This research study is based on the number of repetitions of single and tandem axles of different loads. A single 18 kips axle is used as the standard axle load configuration.

2.12 Failure Mechanisms

The failure mechanisms which are used to study pavement performance are described in the following paragraphs.

2.12.1 Fatigue Cracking

Fatigue cracking is one type of load-associated structural failure. There are two forms of fatigue cracking, top-down and bottom-up. Bottom-up fatigue cracking is governed by the maximum horizontal tensile strain at the bottom of the HMA. Bottom-up begins at the bottom and propagates upward. It is widely accepted as a distress mode which predominantly occurs in

thicker asphalt layers (4 inches or greater). Top-down fatigue cracking begins at the surface of the pavement and propagates downward (ERES 2002).

For the purpose of this research, the failure criterion for pavement in terms of fatigue cracking is 10 percent. Fatigue life is represented in terms of numbers of load repetitions for the pavement to reach failure in terms of fatigue cracking (Huang 2004). The ratio of the actual number of load repetitions to the allowable number of load repetitions is a factor known as damage ratio, which is computed for each load in all seasons and is accumulated over time.

Fatigue damage occurs in two phases, crack initiation and crack propagation (Ayres and Witczak 1998). The number of repetitions for crack initiation is the number of load repetitions needed for a small visible crack to originate. The laboratory fatigue equation used in this research was obtained by the Asphalt Institute in 1982 and is shown in Equation 2.1 (Asphalt Institute 1982). The parameters used in this equation were determined in the laboratory using fatigue beam tests with constant stress or constant strain control. However, these parameters need to be adjusted in order to represent actual field conditions.

$$N_f = 0.00432 * C * \beta_1 k_1 \left(\frac{1}{\epsilon_t} \right)^{k_2 \beta_2} \left(\frac{1}{E} \right)^{k_3 \beta_3} \quad (2.1)$$

Where,

$$C = 10^M$$

$$M = 4.84 \left(\frac{V_b}{V_a + V_b} - 0.69 \right)$$

N_f	=	number of repetitions for fatigue cracking
ϵ_t	=	maximum tensile strain at the bottom of asphalt layer
E	=	dynamic modulus of the asphalt layer
V_a	=	percentage air voids
V_b	=	percentage volume of effective bitumen
k_1	=	-0.00432
k_2	=	3.9492
k_3	=	1.281
$\beta_1, \beta_2, \beta_3$	=	Calibration constants

Crack propagation is the phase during which the number of repetitions for the pavement to reach failure after crack initiation has taken place is obtained. For the purpose of this research, the failure criterion was 10 percent cracking.

2.12.2 Rutting

Rutting is composed of depressions in the wheel path of the pavement surface that occur due to volume change as well as plastic flow in one or more pavement layers (ERES 2002), and is typically considered to be a load-related distress. In the case of bituminous materials, the permanent strain is assumed to be proportional to the resilient strain, as shown in Equation 2.2 (NCHRP 2002), the parameters of which were obtained from laboratory tests. These parameters should be adjusted to estimate actual field conditions using the calibration factors (Harichandran et al. 1989). The permanent vertical strain, ε_p , can be determined by substituting the average vertical compressive strain, ε_r , in the asphalt layer computed by a multi-layer linear elastic program (Groenendijk et al. 1997).

$$\frac{\varepsilon_p}{\varepsilon_r} = \alpha_1 10^{k_1} T^{\alpha_2 k_2} N^{\alpha_3 k_3} \quad (2.2)$$

Where,

ε_p	=	permanent strain
ε_r	=	resilient strain
T	=	AC temperature
N	=	number of load repetitions
k_1	=	-3.51108
k_2	=	1.5606
k_3	=	0.4791 and
$\alpha_1, \alpha_2, \alpha_3$	=	Calibration factors

The equation used for the permanent deformation of unbound materials is given as Equation 2.3.

$$\delta_a(N) = \beta k_1 \varepsilon_v h \left(\frac{\varepsilon_0}{\varepsilon_r} \right) \left(e^{-\left(\frac{\rho}{N}\right)^\beta} \right) \quad (2.3)$$

Where,

δ_a	=	permanent deformation of the unbound layer
N	=	number of repetitions
ε_v	=	average vertical strain
h	=	thickness of the layer
ε_r	=	resilient strain
$\varepsilon_0, \beta, \rho$	=	regression parameters
k_1	=	$\begin{cases} 2.2 & \text{granular materials} \\ 8 & \text{fine grains} \end{cases}$

2.12.3 Thermal Cracking

Two types of cracking are possible due to the influence of climate on asphalt pavements, low-temperature cracking and thermal fatigue cracking. Low-temperature cracking occurs when the ambient temperature is low enough to produce tensile stresses in the asphalt layer (due to contraction) that exceed the material tensile strength. This causes a transverse crack in the pavement layer (ERES 2002).

Thermal fatigue cracking is caused by tensile strain in the asphalt layer due to daily temperature fluctuations (Huang 2004). The thermal cracking model — based on the Superpave Performance Models developed for the Strategic Highway Research Program (SHRP) (Lytton et al. 1993) — estimates thermal cracking as a function of temperature and time of loading. The equation that is used is given as Equation 2.4 (Huang 2004).

$$C_f = \gamma_t \gamma_1 N_0 (\log(C/h_{ac}) / \sigma) \quad (2.4)$$

Where,

C_f	=	observed amount of thermal cracking
γ_1	=	calibration factor based on LTPP data
N_0	=	standard normal distribution
C	=	predicted crack depth by a crack propagation model
h_{ac}	=	thickness of AC layer
σ	=	standard deviation of the log crack depth
γ_t	=	field calibration factor

2.12.4 Roughness

Pavement roughness is described as irregularities in the pavement surface that adversely affect ride quality (WSDOT 1998), and is represented in terms of the distortion of pavement surface, which contributes to an undesirable or uncomfortable ride (Haas and Hudson 1978). Roughness is defined as the deviation of a surface from a true planar surface with characteristic dimensions that affect vehicle dynamics and ride quality (OHPI 2003).

Roughness is measured using the International Roughness Index (IRI), which is a statistic used to estimate the amount of roughness in a measured longitudinal profile. IRI broadly represents the effects of roughness on vehicle response and the user's perception over a range of wavelengths of interest (OHPI, 2003). Evaluation is by increments as shown in Equation 2.5 (ERES 2002).

$$\text{IRI} = \text{IRI}_0 + \Delta\text{IRI} \quad (2.5)$$

Where,

ΔIRI	=	Function (D_j , S_f)
IRI_0	=	pavement roughness when it is newly constructed
D_j	=	effect of surface distress
S_f	=	effect of non-distress variables or site factor

2.13 Road Traffic and Axle Loading

Two main types of traffic data are collected:

1. axle load and configurations, and
2. number and types of vehicles over a period of time.

The data on axle loads and configurations is collected by means of weigh-in-motion (WIM) systems. Automatic vehicle classification (AVC) systems can be used to collect data on the number and types of vehicles over a period of time (ERES 2002).

2.13.1 Traffic Volume

The mechanistic-empirical design approach used in this research considers the following three design levels of traffic inputs (ERES 2002):

1. Level 1 — traffic volume and axle load spectra for a particular project are needed. Traffic data, including the number of trucks in each lane, lane direction, and axle load distribution, need to be determined for the first year following construction (ERES 2002). In order to determine traffic variations with time, the following information is needed:
 - A. AADTT,
 - B. direction distribution factor,
 - C. lane distribution factor, (accounts for the percentage of trucks in the design lane),
 - D. Truck Traffic Distribution Factor (TTDF) (the percent of AADTT for each vehicle type),
 - E. monthly truck traffic adjustment factors by class (used to adjust the AADTT into Monthly Average Daily Truck Traffic (MADTT)), and
 - F. hourly distribution factors (used to distribute the MADTT volumes by hour of the day).
2. Level 2 — uses the same traffic data as Level 1, except that instead of the facility-specific axle load spectra data, regional axle load spectra data are used. In order to accurately measure truck volumes, including weekend traffic volume variations and significant seasonal trends in truck load, Level 2 requires collecting sufficient truck volume data on a given facility. In order to differentiate between routes with heavy weights and those with light weights, vehicle weights are taken from vehicle weight summaries, which are maintained by each state (ERES 2002).
3. Level 3 — used when the designer has only the AADTT and the percentage distribution of the trucks for a particular roadway section under study. Level 3 uses regional or state default classification and axle load spectra data (ERES 2002).

2.13.2 Types of Vehicles

Pavement structural damage caused by small axle loads imposed by cars and light panel trucks is negligible. It is the heavier axle loads associated with larger commercial vehicles that cause damage to pavements (Luskin and Walton 2001). For this reason, all U.S. states now assign a maximum axle load limit and a maximum gross vehicle weight for use on their highway networks. For example, the maximum legal allowable weight for a five-axle semi-trailer truck in Texas is 80,000 lbs. (TxDOT 2004).

Texas divides the types of vehicles into fifteen categories, as shown in Figure 2.3. FHWA classifies the vehicles into thirteen categories, as illustrated in Figure 2.4.

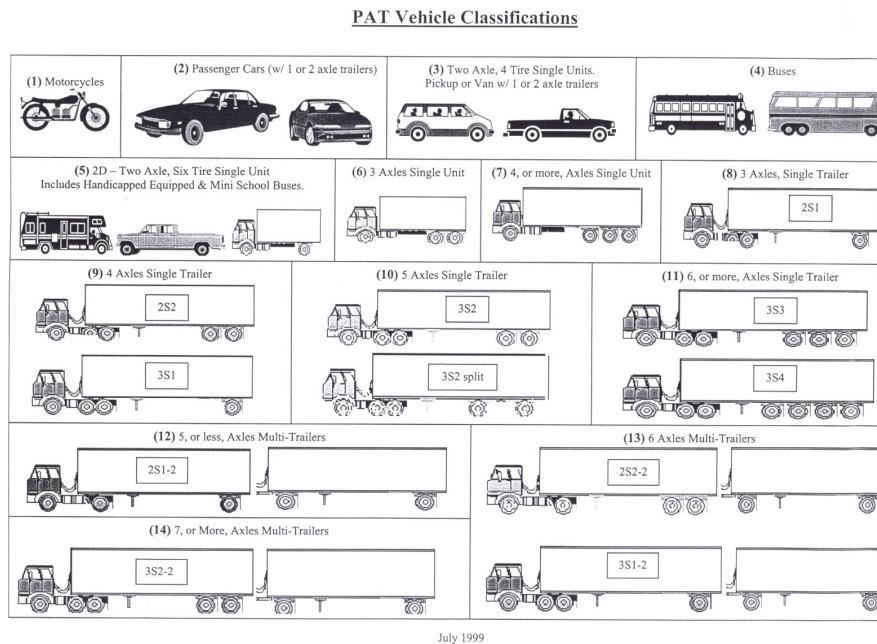


Figure 2.3: Texas Vehicle Classification

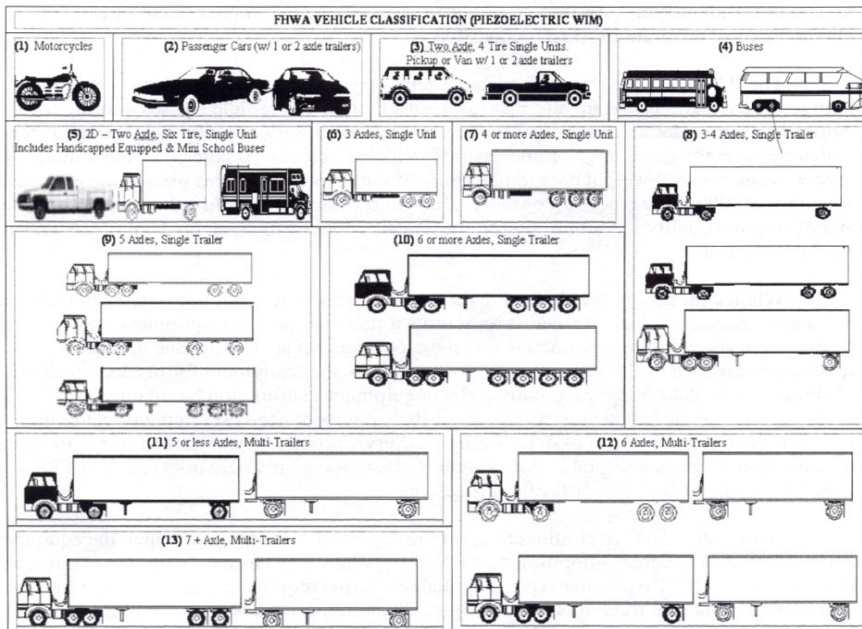


Figure 2.4: FHWA Vehicle Classification

CHAPTER 3. EXPERIMENTAL SET-UP AND METHODOLOGY

3.1 Experimental Set-up

For the purpose of this research study, six pavement structures were analyzed, which are described in greater detail in Section 3.1.2. The major input variables for the experiment are now discussed.

3.1.1 Environmental Conditions

In order to analyze the performance of the pavement structures under varied climatic conditions, five different locations were selected in Texas (as shown in Table 3.1 and Figure 3.1).

Table 3.1: Test Locations

Code	Station	Latitude (deg.min)	Longitude (deg.min)	Elevation (ft)
AUS	Austin	30.19	-97.46	648
AMA	Amarillo	35.13	-101.43	3586
DFW	Dallas/Fort Worth	32.54	-97.02	559
ELP	El Paso	31.49	-106.23	3942
IAH	Houston Intercontinental Airport	29.59	-95.22	118

The rationale behind the selection of the locations was to represent different geographical locations and varying climatic conditions existing in Texas. Following are the locations and the types of weather conditions prevailing at these stations:

1. Amarillo (AMA-dry/cold): represents the Texas Panhandle region, with dry cold weather and high elevation. The average high temperature in Amarillo is 92°F (34°C) in summer and the average low is 22°F (-4°C) in winter, with annual rainfall of 19.5 inches (495.3 mm) (ACVC 2002).
2. Austin (AUS-mixed): represents Central Texas, with an average high temperature of 98°F (37°C) in summer and an average low temperature of 42°F (7°C) in winter, with an annual rainfall of 32.5 inches (825.5 mm) (GACC 2003).

3. Dallas/Fort Worth (DFW-wet/cold): represents wet and cold weather in Texas. Dallas has a average high temperature of 100°F (37°C) in summer and an average low temperature of 33°F (0°C) in winter, with annual rainfall of 32 inches (812.8 mm) (Yahoo! Inc. 2003a).
4. El Paso (ELP-dry/warm): in Southwest Texas bordering Mexico, represents dry, warm weather. Temperatures in El Paso vary from 97°F (37°C) to 64°F (18°C) in summer and from 56°F (14°C) to 29°F (-1°C) in winter, with annual rainfall of 8.65 inches (219.7 mm) (DUDWMI 2003).
5. Houston (IAH-wet/warm): located along the Gulf of Mexico, represents hot and humid weather. Houston has an average high temperature of 90°F (32°F) in summer and an average low temperature of 40°F (4°F) in winter, with annual precipitation of 46.07 inches (1170.2 mm) (Yahoo Inc. 2003b).

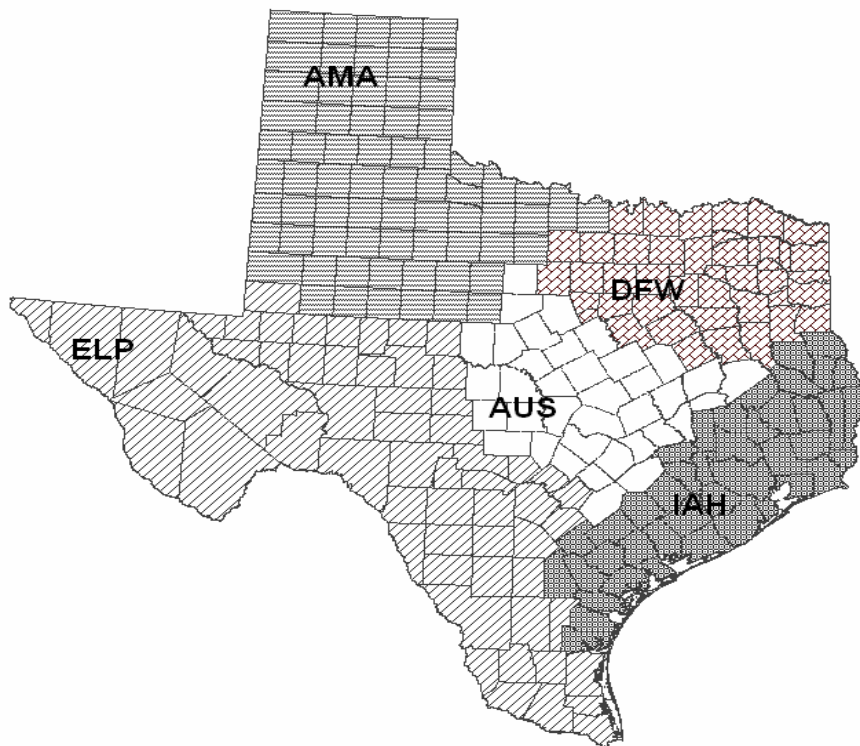


Figure 3.1: Experimental Locations

3.1.2 *Pavement Structures*

The six pavement structures selected for experimentation were constructed of the following materials:

1. Asphalt surface: a mixture of dense-graded crushed dolomitic limestone aggregate of $\frac{3}{4}$ -inch maximum size, and natural sand with about 5.4 percent of 85-100-penetration-grade paving asphalt (AASHO 1962).
2. A-1-b base: gravel base of $1\frac{1}{2}$ -inch maximum size crushed dolomitic limestone and a maximum dry density of 140 pcf (AASHO 1962).
3. A-2-4 subbase: sand gravel material containing small amounts of fine sand and friable fine-grained soil of 1-inch maximum size and a maximum dry density of 138 pcf (AASHO 1962).
4. A-6 subgrade: plastic clay soil having 75.5 percent passing the 0.075-mm (No. 200) sieve, and 96.6 percent passing the 4.75-mm (No. 4) sieve. The maximum dry unit weight of the material was 116.4 pcf (AASHO 1962).

The particle size distribution of the materials is shown in Figure 3.2. Table 3.2 shows the pavement layers.

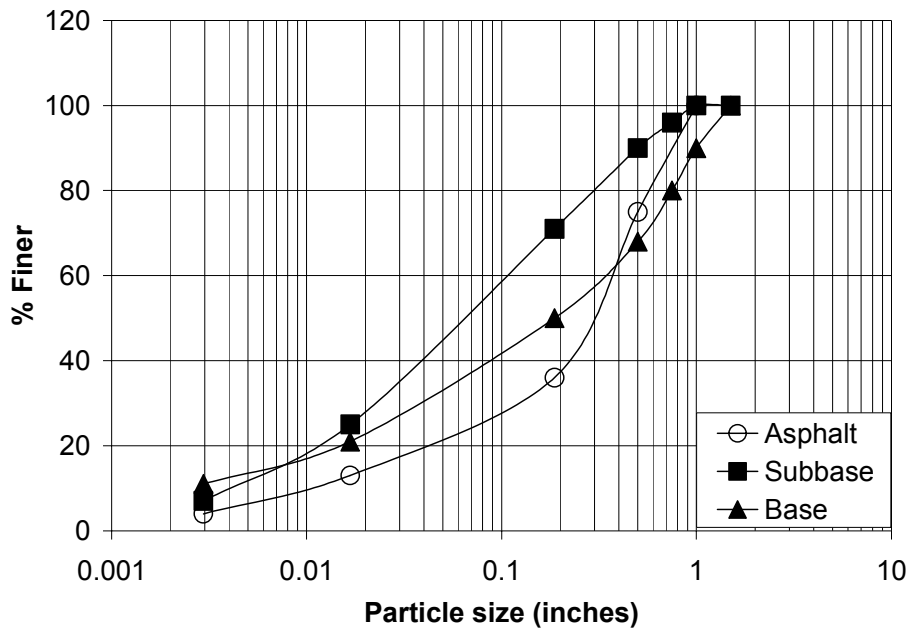


Figure 3.2: Gradation Curve for Different Materials (AASHO 1962)

The materials were selected in order to be consistent with the AASHO Road Test experiment (AASHO 1962). Hence, pavement performance can be evaluated by comparing pavement designed by the empirical method (AASHTO 1993) and the mechanistic-empirical method (NCHRP 2002), with the exception of the subgrade layer, whose resilient modulus was selected to be more consistent with Texas conditions.

Different layer thicknesses were then selected for the six structures as shown in Table 3.3. Using the layer strength coefficients (a value) given in Table 3.2 and the layer thicknesses from Table 3.3, the structural numbers (SN) for the six structures were calculated using Equation 3.1 (Huang 2004), and are also given in Table 3.3.

Table 3.2: Pavement Layers

Layer	Material	a	Modulus(psi)
Surface	Dense Asphalt	0.44	
Base	A-1-b	0.14	75,000
Subbase	A-2-4	0.11	45,000
Subgrade	A-6	-	8,000

Table 3.3: Layer Thicknesses

Layer	Structures					
	#1	#2	#3	#4	#5	#6
Surface	2	2	4	4	6	6
Base	6	9	6	9	6	9
Subbase	4	8	8	8	8	12
Subgrade	Semi-infinite	Semi-infinite	Semi-infinite	Semi-infinite	Semi-infinite	Semi-infinite
Structural Number	2.16	3.02	3.48	3.9	4.36	5.22

SN = Structural Number of the pavement

$$SN = a_1D_1 + a_2D_2 + a_3D_3 \quad (3.1)$$

Where,

- a_1 = layer coefficient for surface
- a_2 = layer coefficient for base
- a_3 = layer coefficient for subbase
- D_1 = asphalt surface thickness
- D_2 = base thickness
- D_3 = subbase thickness

3.1.3 Traffic Volume

Once the pavement structures were designed and their SN calculated, the expected traffic volumes were calculated using the empirical design Equation 3.2 (AASHTO 1993). The development of this equation was based primarily on the results of the AASHTO Road Test and expresses the expected design traffic (in ESALs) as a function of the SN, allowable change in pavement serviceability index (Δ PSI), resilient modulus of the subgrade (M_R), and reliability.

$$\log W_{18} = Z_R S_0 + 9.36 \log(SN + 1) - 0.20 + \frac{\log[\Delta PSI / (4.2 - 1.5)]}{0.4 + 1094 / (SN + 1)^{5.19}} + 2.32 \log M_R - 8.07 \tag{3.2}$$

Where,

- W_{18} = Number of 18 kips single axle load applications
- = Equivalent Single Axle Load (ESALs)
- SN = Structural Number of the pavement
- ΔPSI = Pavement Serviceability Index = $p_0 - p_f$
- Z_R = Normal Deviate for a given reliability R
- S_0 = Standard Deviation

For the purpose of this research, 50 percent reliability is used, for which the Z_R value is 0, and a p_0 value of 4.4 and p_f value of 2.5 are used, which gives a ΔPSI of 1.9. The expected ESALs obtained for the six structures are given in Table 3.4. Using these design ESALs, AADTT values are calculated assuming a design life of 20 years with no growth in traffic. Another assumption was made that, on average, each truck is approximately equivalent to one ESAL.

Table 3.4: Empirical Traffic Volumes

Structure	Structural Number	ESAL	Daily ESAL
#1	2.16	259,661	36
#2	3.02	2,058,528	282
#3	3.48	5,044,782	691
#4	3.9	10,545,546	1,445
#5	4.36	22,229,574	3,045
#6	5.22	79,273,063	10,859

3.1.4 Axle Loads

The axle load spectra is the distribution of axle loads for single, tandem, tridem, and quad axles as a percentage of the total number of single, tandem, tridem, and quad axles respectively (ERES 2002). For the purpose of this research study, the structures are simulated for single and tandem axles only, as shown in Table 3.5.

Table 3.5: Axle Loads Used in this Research

Single (kips)	Tandem (kips)
12	26
15	30
18	34
21	38
24	42

3.2 Methodology

After the experimental locations were chosen, the six pavement structures were designed, design ESAL values were calculated, and daily traffic was estimated for the various structures in order for the pavements to reach failure in terms of rutting and fatigue cracking at the end of the performance period. The failure criteria were chosen as 0.5 inches of rutting and 10 percent fatigue cracking. A performance period of 20 years was used for the analysis.

“Empirical AADTT” values were obtained based on the AASHTO 1993 Design Guide, as given in Table 3.4. Using these empirical values, the structures were analyzed for failure in terms of rutting and fatigue cracking performance. It was observed that pavement deterioration was slowest in Amarillo as compared to the other four locations. Hence it was decided to use Amarillo as the test location, and the smallest axle load of 12 kips single axle was used to determine the “mechanistic AADTT values” for the six structures. It should be noted that these “mechanistic-based AADTT” values are expressed in single axles rather than actual trucks.

The traffic volume needed to reach failure was compared with the empirical traffic volumes given in Table 3.4. If the failure was not obtained as predicted, the AADTT values were adjusted to reach failure as predicted. Reviewing the results it was observed that for a given AADTT value, even though a pavement reached 0.5-inch rutting, fatigue cracking was well below 10 percent. The results necessitated the need to use different AADTT values for the analysis of pavement failure in terms of rutting and fatigue cracking for a given structure. The AADTT values which were selected to evaluate the failure in terms of rutting and fatigue cracking are given in Table 3.6.

Table 3.6: AADTT Values for the Pavements to Reach Failure in Terms of Rutting and Fatigue Cracking

Structure	Structural Number	AADTT	
		Rutting	Fatigue Cracking
1	2.16	3,000	25,000
2	3.02	3,800	25,000
3	3.48	3,600	25,000
4	3.9	2,400	25,000
5	4.36	5,000	25,000
6	5.22	2,600	25,000

In the last part of this research study, pavement life is evaluated relative to the life under the standard 18 kips single axle load. Since load repetitions indicate the pavement life for different axle loads, the pavement life varies under different axle loads making it difficult to determine generalized trends. This analysis was carried out by applying the EDF concept developed in South Africa (Prozzi and de Beer 1997).

CHAPTER 4. RESULTS AND ANALYSIS

4.1 Results

Six pavement structures were analyzed for each of the five locations. A total of thirty different conditions were evaluated under five different single axle loads and five different tandem axle loads. Pavement performance was evaluated in terms of rutting and fatigue cracking. Other failure mechanisms which were evaluated but not considered for analysis were thermal cracking and roughness because unrealistic performance predictions were obtained. For example, roughness values in some cases changed from 61 inches/mile at the beginning of the performance period to 63 inches/mile at the end of the 20-year performance period, which was a negligible change in 20 years.

Table 4.1 shows the ESAL values based on empirical and mechanistic-empirical values for rutting and fatigue for 18-kips single axle load at the Amarillo site. The mechanistic-empirical approach estimated longer pavement life for structures 1 and 2 compared to the empirical design values based on the AASHTO 1993 design guide. For structure 3, mechanistic-empirical and empirical values are comparable. On the other hand, for structures 4, 5 and 6, the mechanistic-based analysis estimates longer pavement life in terms of fatigue and shorter pavement life in terms of rutting compared to the empirical-based design life. The failure criterion in the AASHTO 1993 design guide is based on riding quality in terms of Pavement Serviceability Index (PSI), and the failure criteria used in the mechanistic-empirical approach are in terms of rutting and fatigue cracking. As the SN increases, the empirical pavement life increases, whereas the mechanistic-empirical pavement life initially increases and then decreases.

Table 4.1: Empirical and Mechanistic-Empirical Design Lives

Structure	Empirical AASHTO 1993	Mechanistic-Empirical (AMA-18 kips)	
	PSI	Rutting	Fatigue
1	259,661	4,118,070	81,325,200
2	2,058,528	5,517,100	40,405,800
3	5,044,782	4,215,900	3,253,010
4	10,545,546	4,927,220	26,747,000
5	22,229,574	5,204,810	22,048,200
6	79,273,063	5,826,500	76,265,000

4.1.1 Rutting

Table 4.2 indicates the number of axle repetitions for each structure to reach 0.5-inch rutting in the case of single axle loads.

Table 4.2 Rutting Life for Single Axle Loads

Location	Structure	Single Axle Load (lbs.)				
		12,000	15,000	18,000	21,000	24,000
AMA	S1	10,322,900	7,243,360	5,118,070	3,643,370	2,602,410
	S2	12,335,400	8,015,410	5,517,100	3,747,470	2,498,310
	S3	11,784,800	5,360,960	4,215,900	3,070,840	2,446,260
	S4	8,258,300	6,176,380	4,927,220	4,059,750	3,261,680
	S5	7,477,500	6,650,590	5,204,810	4,192,770	3,469,880
	S6	8,946,490	7,179,750	5,826,500	4,886,740	4,059,750
AUS	S1	5,031,320	3,469,880	2,428,910	1,778,310	1,387,950
	S2	5,465,050	3,174,940	2,342,170	1,769,640	1,197,110
	S3	3,070,840	2,498,310	2,290,120	1,821,680	1,717,590
	S4	3,678,070	2,880,000	2,116,620	1,700,240	1,596,140
	S5	3,469,880	3,325,300	2,530,120	2,457,830	2,240,960
	S6	4,022,160	3,458,310	2,668,910	2,180,240	1,804,340
DFW	S1	8,284,330	5,681,920	4,120,480	3,036,140	2,081,930
	S2	9,212,520	5,621,200	3,799,510	2,498,310	1,821,680
	S3	4,996,620	4,111,800	3,018,790	2,394,210	1,821,680
	S4	5,655,900	4,163,850	3,296,380	2,810,600	2,116,620
	S5	5,927,700	4,337,340	3,469,880	3,180,720	2,530,120
	S6	6,315,170	5,300,230	4,022,160	3,533,490	3,082,410
ELP	S1	5,725,290	3,686,740	2,602,410	1,908,430	1,344,580
	S2	6,297,820	3,799,510	2,498,310	1,769,640	1,145,060
	S3	4,163,850	3,070,840	2,394,210	1,821,680	1,301,200
	S4	4,510,840	3,365,780	2,775,900	2,186,020	1,665,540
	S5	4,409,630	3,325,300	2,602,410	2,024,090	1,662,650
	S6	4,924,330	3,984,570	3,120,000	2,631,320	2,255,420
IAH	S1	6,722,880	4,163,850	2,992,770	1,995,180	1,431,320
	S2	7,338,790	4,267,950	2,498,310	1,821,680	1,249,160
	S3	4,944,570	3,695,420	2,966,740	2,290,120	1,821,680
	S4	5,378,310	4,094,450	3,296,380	2,775,900	2,047,230
	S5	5,927,700	4,265,050	3,397,590	2,602,410	2,530,120
	S6	6,277,580	4,999,510	4,022,160	3,495,900	3,007,230

Figure 4.1 represents rutting as a function of the SN of the various structures, using 18 kips standard single axle load.

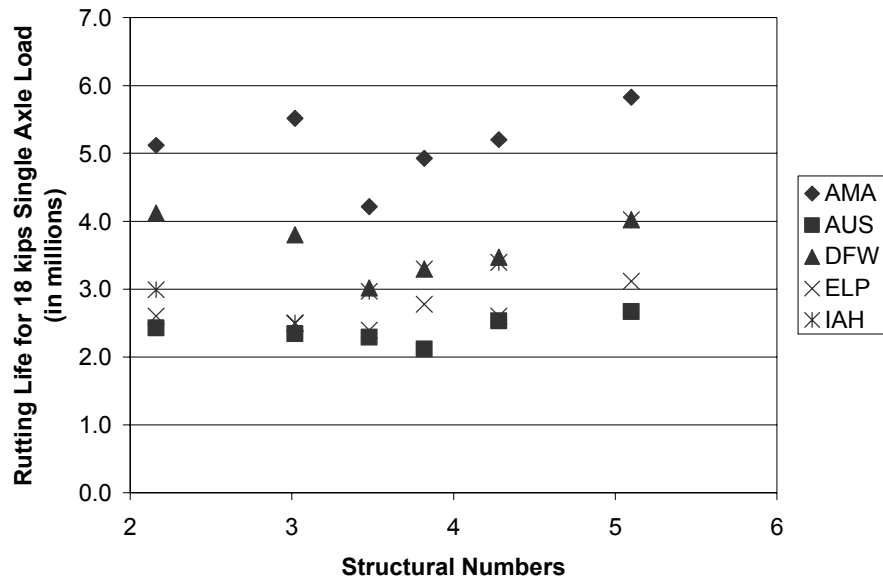


Figure 4.1: Rutting Life for 18 kips Standard Single Axle Load

Figure 4.1 illustrates that as the SN is increased, the rutting life decreases; after a certain “critical” value of the SN, as the SN is further increased, rutting life increases. Hence, pavement performance deteriorates initially as the SN increases, but with a further increase in the SN, pavement performance improves after the critical value of the SN.

Rutting life for single axle loads for the six structures at each location is shown in Figures 4.2 to 4.7. The figures indicate that as axle loads increase from 12,000 lbs. to 24,000 lbs., the number of axle load repetitions required for the pavements to reach 0.5-inch rutting is reduced from 12,300,000 (AMA S2) to 1,145,000 (ELP S2), implying increased pavement deterioration.

While everything else remains constant, of the five stations, Amarillo requires the highest number of repetitions to reach 0.5-inch rutting, indicating slow deterioration in terms of rutting in Amarillo. Austin and El Paso achieved 0.5-inch rutting with the least number of axle repetitions

compared to the other locations. Thus, of the five stations, the fastest pavement deterioration in terms of rutting occurs in Austin and El Paso, which could be attributed to the warmer climate prevailing in these areas. The slow pavement deterioration in Amarillo can be attributed to cold weather conditions that prevailing in the area.

The number of tandem axle load repetitions for each structure to reach 0.5-inch rutting is tabulated in Table 4.3.

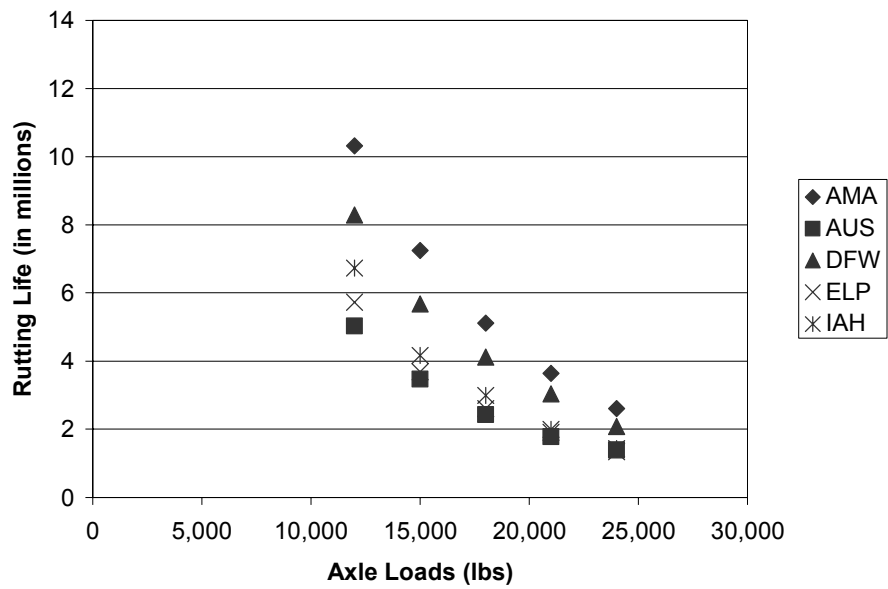


Figure 4.2: Rutting Life of Structure 1 for Single Axle Loads

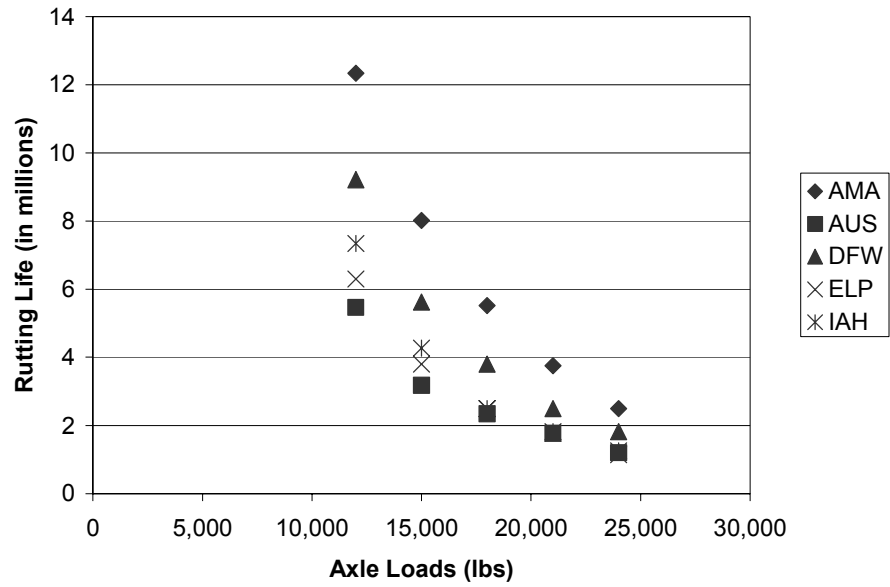


Figure 4.3: Rutting Life of Structure 2 for Single Axle Loads

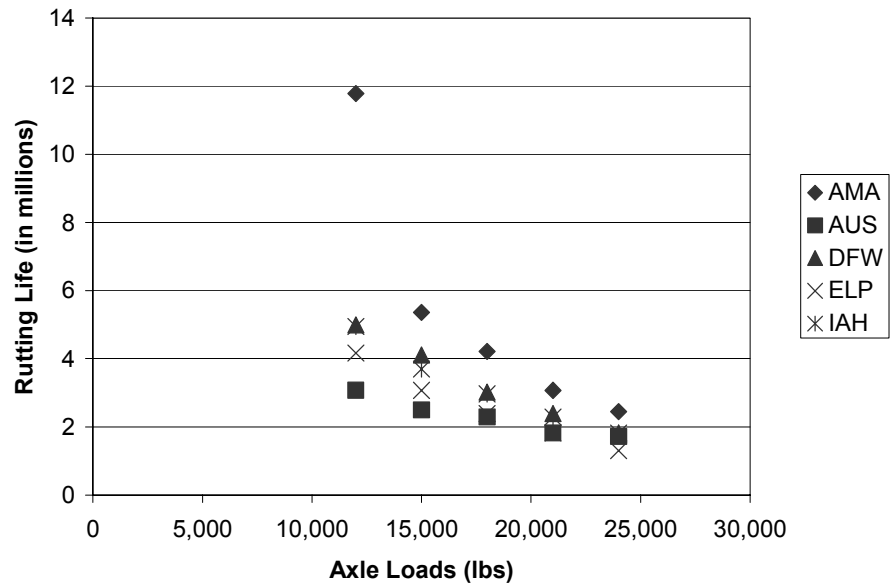


Figure 4.4: Rutting Life of Structure 3 for Single Axle Loads

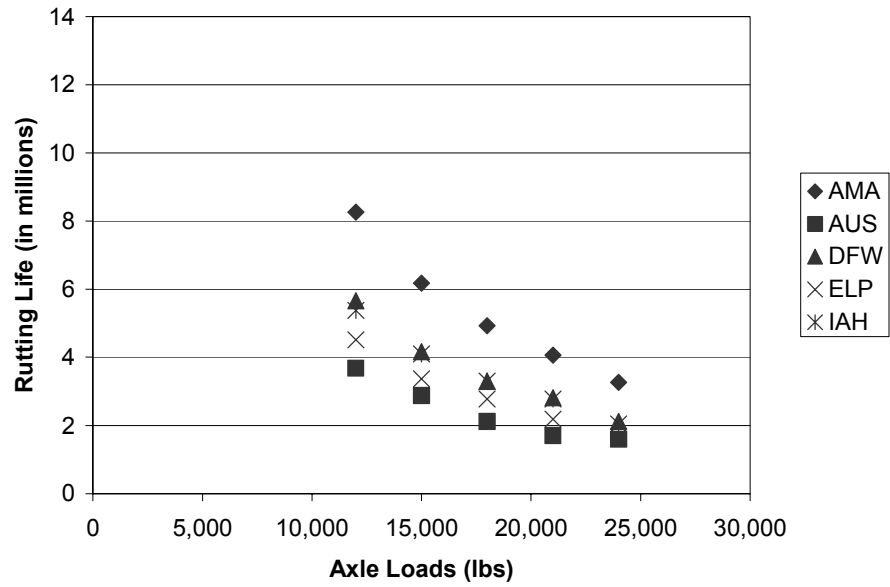


Figure 4.5: Rutting Life of Structure 4 for Single Axle Loads

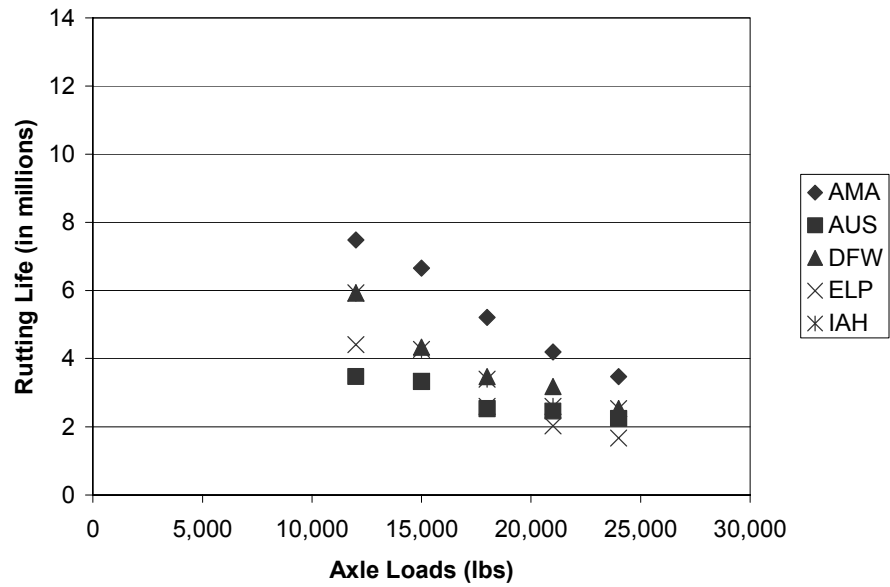


Figure 4.6: Rutting Life of Structure 5 for Single Axle Loads



Figure 4.7: Rutting Life of Structure 6 for Single Axle Loads

Table 4.3: Rutting Life for Tandem Axle Loads

Location	Structure	Tandem Axle Load (lbs.)				
		26,000	30,000	34,000	38,000	42,000
AMA	S1	3,253,010	2,515,660	1,995,180	1,474,700	1,040,960
	S2	4,163,850	2,966,740	2,290,120	1,665,540	1,197,110
	S3	2,446,260	1,821,680	1,561,440	1,145,060	1,093,010
	S4	2,845,300	2,394,210	2,012,530	1,630,840	1,492,050
	S5	3,253,010	2,457,830	1,879,520	1,662,650	1,590,360
	S6	3,157,590	2,706,500	2,217,830	2,105,060	1,766,740
AUS	S1	1,648,190	1,431,320	997,589	867,469	563,855
	S2	1,821,680	1,301,200	1,093,010	676,626	572,529
	S3	1,613,490	1,197,110	1,040,960	676,626	624,578
	S4	1,422,650	1,214,460	1,179,760	867,469	798,071
	S5	1,662,650	1,518,070	939,758	867,469	795,180
	S6	1,691,560	1,353,250	1,315,660	1,240,800	902,168
DFW	S1	2,515,660	1,951,800	1,518,070	1,084,340	954,216
	S2	2,602,410	1,873,730	1,509,400	1,145,060	1,093,010
	S3	1,821,680	1,301,200	1,197,110	1,145,060	1,093,010
	S4	1,977,830	1,596,140	1,214,460	1,145,060	832,770
	S5	2,024,090	1,662,650	1,590,360	1,518,070	1,445,780
	S6	2,217,830	1,804,340	1,729,150	1,315,660	1,278,070
ELP	S1	1,908,430	1,344,580	954,216	824,095	520,481
	S2	1,821,680	1,249,160	1,093,010	676,626	572,529
	S3	1,197,110	1,093,010	988,914	624,578	572,529
	S4	1,561,440	1,179,760	832,770	763,373	728,674
	S5	1,518,070	1,373,490	867,469	795,180	722,891
	S6	1,729,150	1,353,250	1,202,890	864,577	826,987
IAH	S1	1,995,180	1,518,070	1,127,710	910,842	693,975
	S2	1,873,730	1,613,490	1,145,060	988,914	624,578
	S3	1,821,680	1,509,400	1,197,110	1,093,010	988,914
	S4	1,769,640	1,492,050	1,214,460	1,179,760	867,469
	S5	2,313,250	1,662,650	1,590,360	1,518,070	1,228,910
	S6	2,180,240	1,766,740	1,428,430	1,315,660	1,278,070

Rutting life plots for tandem axle loads for the six structures at each location are shown in Figures 4.8 to 4.13. It is again observed that as the axle loads increase from 26,000 lbs. to 42,000 lbs., the number of axle load repetitions required for the pavements to reach 0.5-inch rutting is reduced from 4,200,000 (AMA S2) to 520,000 (ELP S1), implying increased pavement deterioration.

While everything the other factors remain constant, amongst the five stations, Amarillo requires the highest number of repetitions to reach 0.5-inch rutting on each of the six structures. Austin and El Paso reach 0.5-inch rutting with the least number of repetitions compared to the other locations.

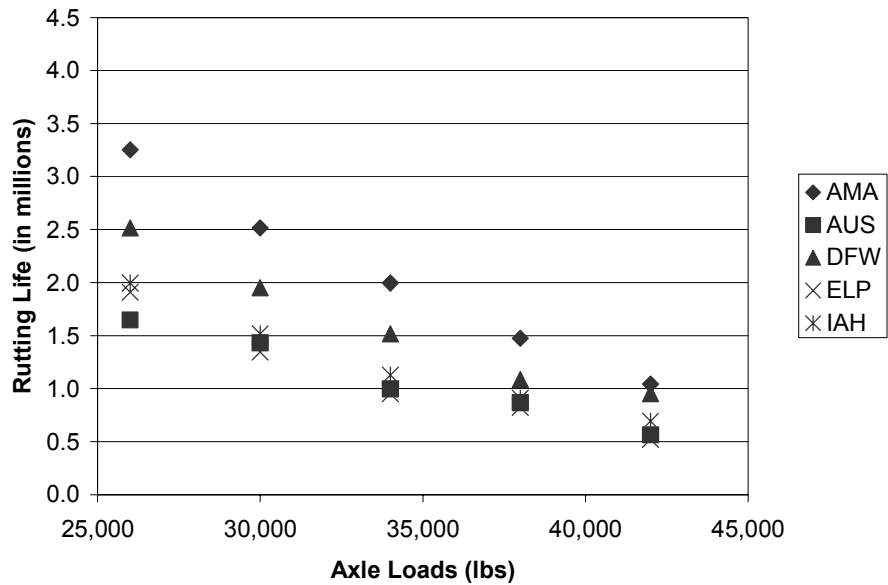


Figure 4.8: Rutting Life of Structure 1 for Tandem Axle Loads

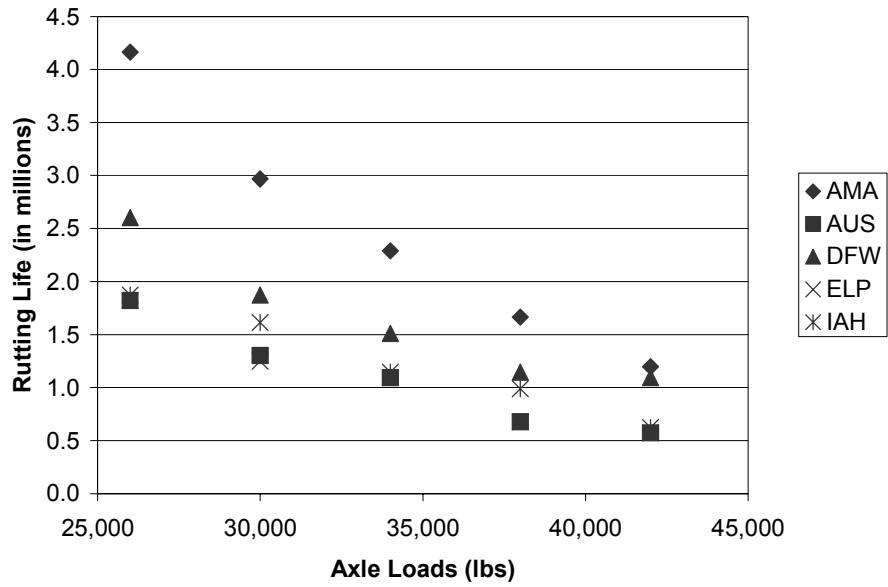


Figure 4.9: Rutting Life of Structure 2 for Tandem Axle Loads

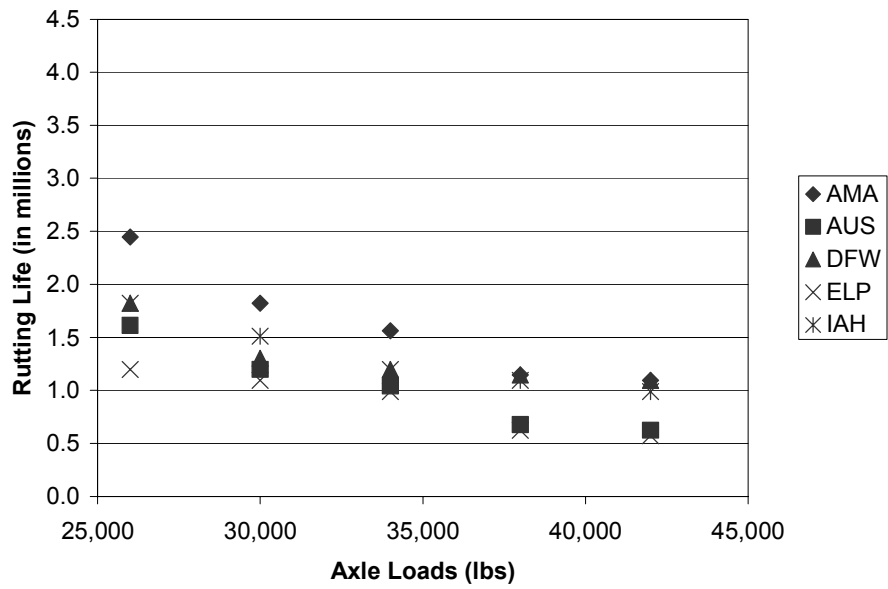


Figure 4.10: Rutting Life of Structure 3 for Tandem Axle Loads

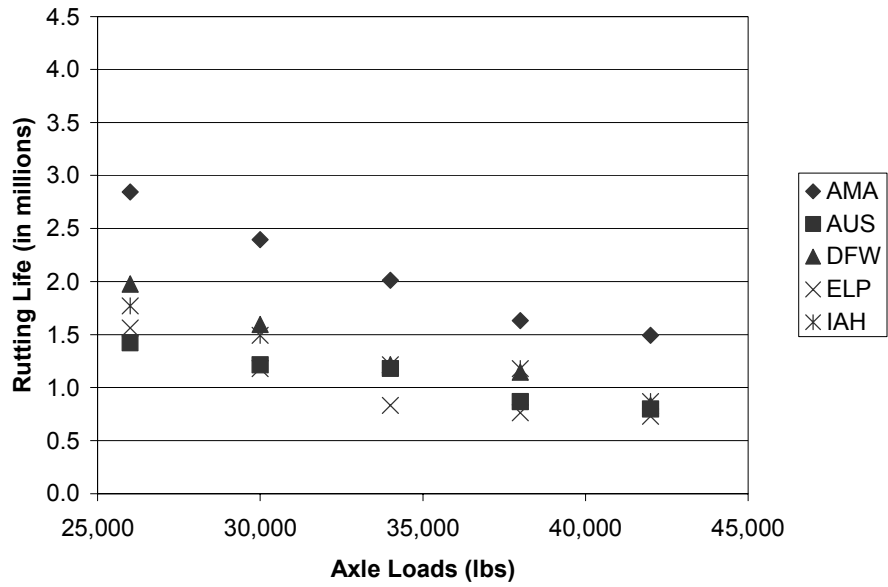


Figure 4.11: Rutting Life of Structure 4 for Tandem Axle Loads

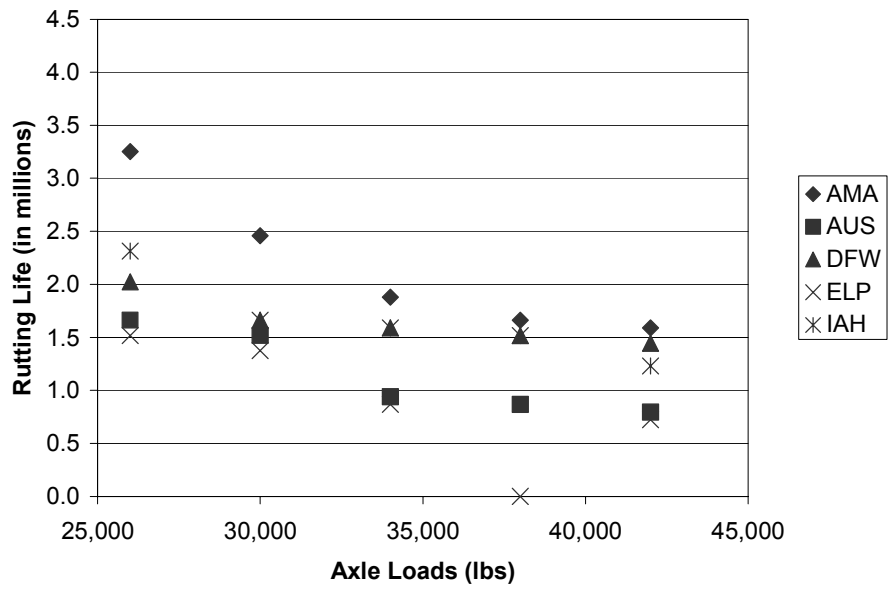


Figure 4.12: Rutting Life of Structure 5 for Tandem Axle Loads

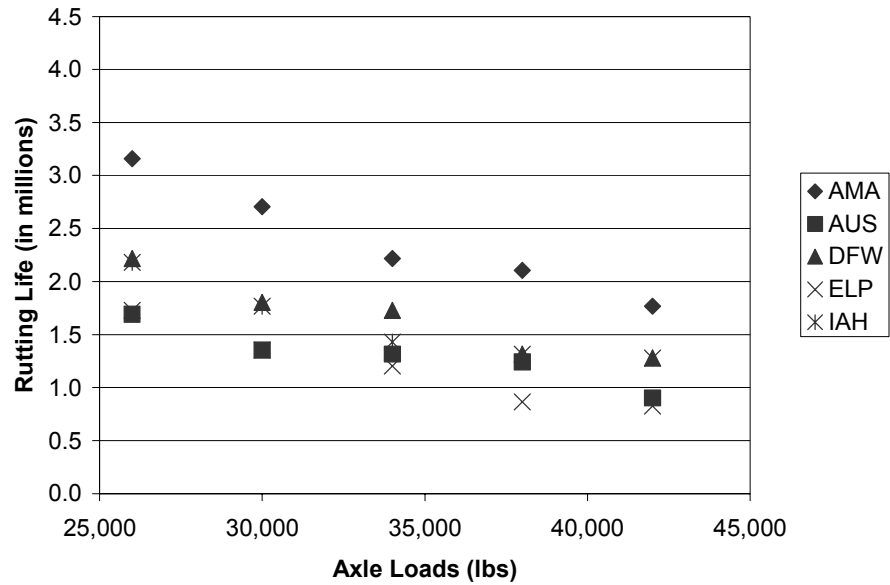


Figure 4.13: Rutting Life of Structure 6 for Tandem Axle Loads

4.1.2 Fatigue Cracking

Results of fatigue cracking indicate that structural deterioration is less than 10 percent fatigue cracking. Fatigue life in terms of the number of single axle load repetitions is given in Table 4.4; the same for tandem axle loads is given in Table 4.5. The blank cells in the tables represent the structures for which 10 percent fatigue cracking was not reached during the 20-year performance period for the 25,000-AADTT value, the maximum possible value available in the Design Guide. The 25,000-AADTT value is a limitation of the Design Guide.

Table 4.4: Fatigue Life for Single Axle Loads

Location	Structure	Single Axle Load (lbs.)				
		12,000	15,000	18,000	21,000	24,000
AMA	S1			81,325,200	58,554,100	44,819,200
	S2		60,608,700	40,405,800	28,421,000	21,230,200
	S3	4,631,300	3,975,900	3,253,010	2,530,120	2,168,670
	S4	86,746,900	46,265,000	26,747,000	16,626,500	10,843,400
	S5		75,180,600	22,048,200	4,337,340	3,614,450
	S6			76,265,000	44,819,200	28,192,700
AUS	S1	80,602,300	50,240,900	33,975,900	24,578,300	19,156,600
	S2	49,993,600	28,078,600	17,121,100	11,984,800	8,902,970
	S3	41,927,700	20,602,400	11,204,800	6,867,460	5,060,230
	S4	43,734,900	22,409,600	13,373,500	8,674,690	5,783,130
	S5		56,024,000	29,277,100	16,626,500	10,481,900
	S6		85,662,500	45,903,600	27,469,800	17,710,800
DFW	S1				86,746,900	68,313,200
	S2	82,181,300	53,075,400	35,269,500	24,654,400	18,490,800
	S3	43,012,000	20,963,800	11,566,300	6,867,460	4,698,790
	S4	44,457,800	22,409,600	13,373,500	8,674,690	5,783,130
	S5		58,192,700	30,361,400	17,349,400	10,843,400
	S6		86,746,900	46,987,900	28,192,700	18,072,300
ELP	S1	80,240,900	37,666,400	32,891,500	23,493,900	18,433,700
	S2	60,266,300	34,242,200	20,887,700	14,724,100	10,615,100
	S3	22,942,300	9,587,810	4,793,910	3,424,220	2,396,950
	S4	44,457,800	22,409,600	13,012,000	8,674,690	5,783,130
	S5		56,385,500	29,277,100	16,987,900	10,481,900
	S6		86,385,400	45,903,600	27,469,800	17,710,800
IAH	S1	78,072,200	48,795,100	32,891,500	24,216,800	18,795,200
	S2	45,199,700	24,312,000	15,066,600	10,272,700	7,533,280
	S3	21,915,000	9,578,100	5,136,330	3,424,220	2,739,380
	S4	42,650,500	21,686,700	13,012,000	8,313,240	5,783,130
	S5		58,192,700	30,361,400	17,349,400	10,843,400
	S6		82,771,000	44,096,300	26,385,500	16,987,900

Figure 4.14 represents fatigue cracking as a function of the SN of the various structures, using 18 kips standard single axle load.

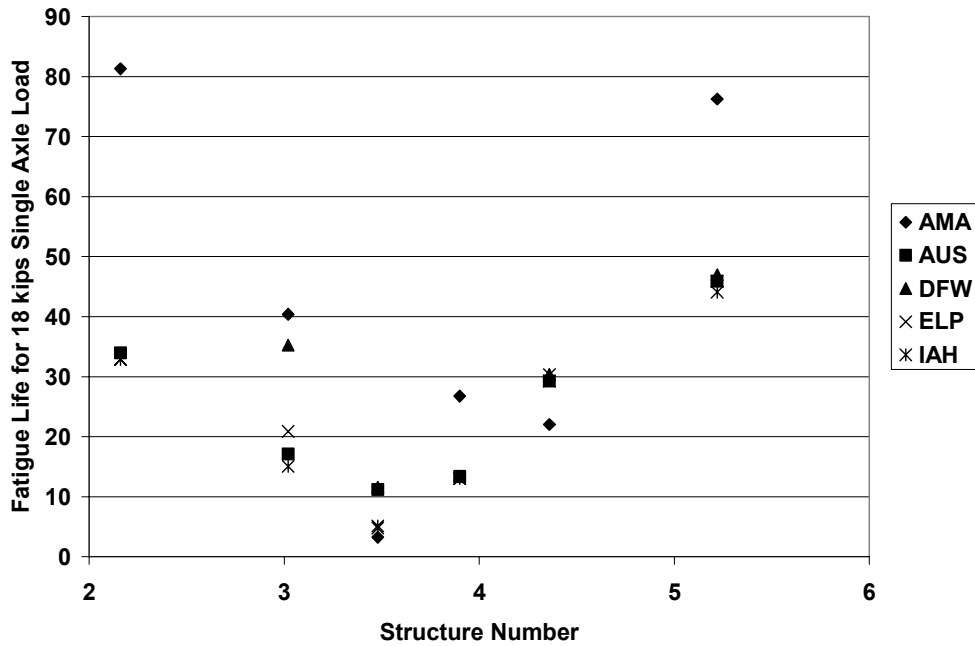


Figure 4.14: Fatigue Life for 18 kips Standard Single Axle Load

Figure 4.14 shows that as the SN is increased the fatigue life decreases; after a “critical” value of the SN, as the SN is further increased, fatigue life increases. Therefore, pavement performance decreases initially as the SN is increased, and as the SN increases, pavement performance improves. The critical SNs are not the same for all environments, but in most cases seem to be between 3.0 and 4.0.

The fatigue life plots of the number of single axle load repetitions for the pavements to reach 10 percent fatigue cracking are given in Figures 4.15 to 4.20 for structures 1 to 6, respectively. The figures indicate that as the load increases from 12,000 lbs. to 24,000 lbs., the number of axle load repetitions reduces from 90,000,000 (AMA S4) to 2,000,000 (ELP S3), implying faster pavement deterioration under heavier axle load configurations.

Fatigue cracking was slowest in Amarillo compared to the other locations for structures 2, 4 and 6, while Dallas experienced the slowest fatigue cracking for structure 1, and Austin the slowest

fatigue cracking for structure 3. Fatigue cracking for structure 5 is similar for all locations except Amarillo, which showed the slowest fatigue cracking.

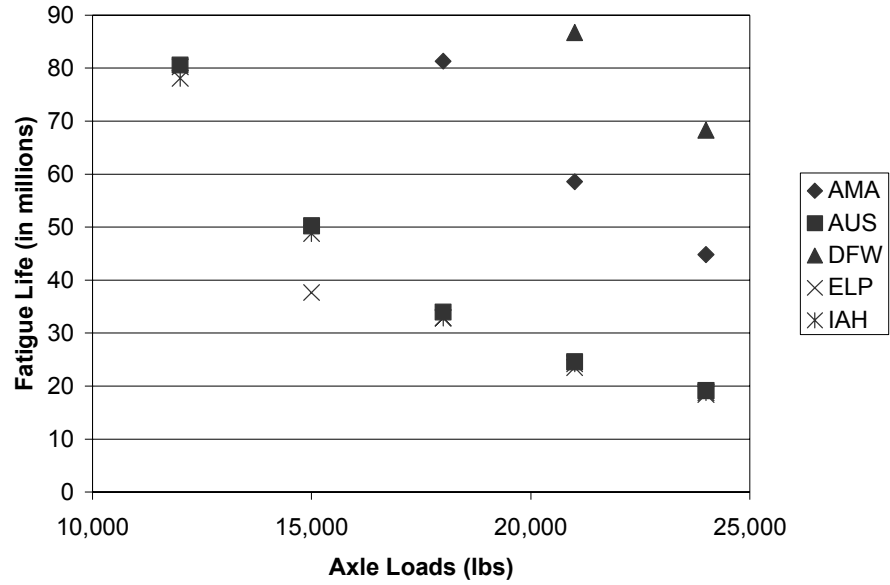


Figure 4.15: Fatigue Life of Structure 1 for Single Axle Loads

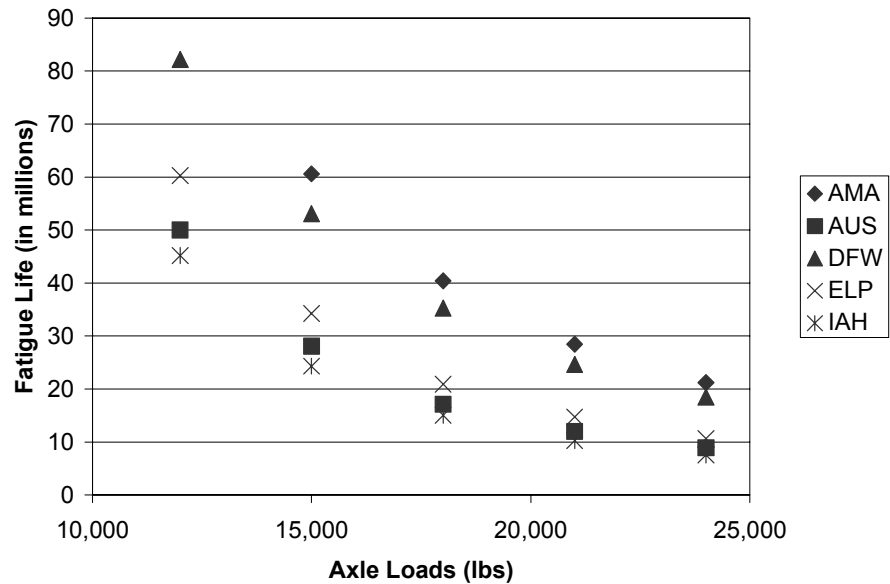


Figure 4.16: Fatigue Life of Structure 2 for Single Axle Loads

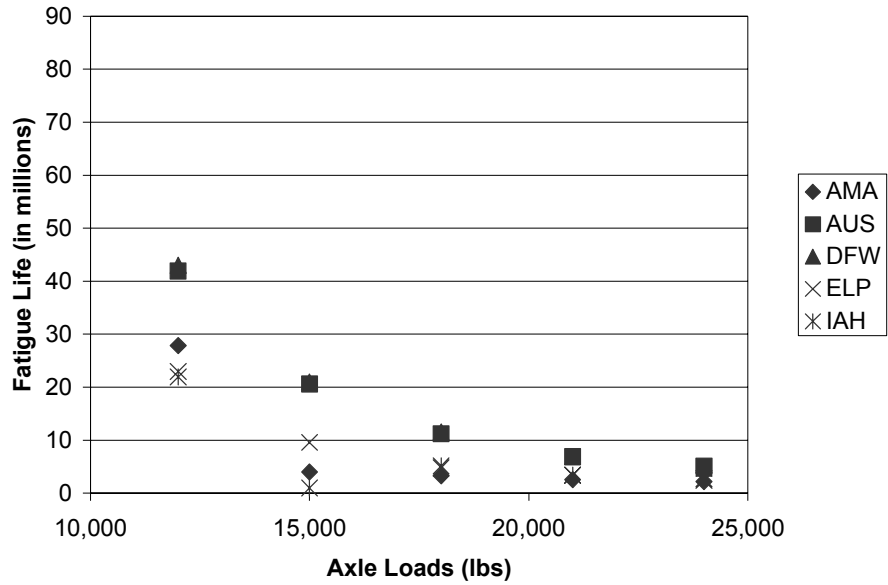


Figure 4.17: Fatigue Life of Structure 3 for Single Axle Loads

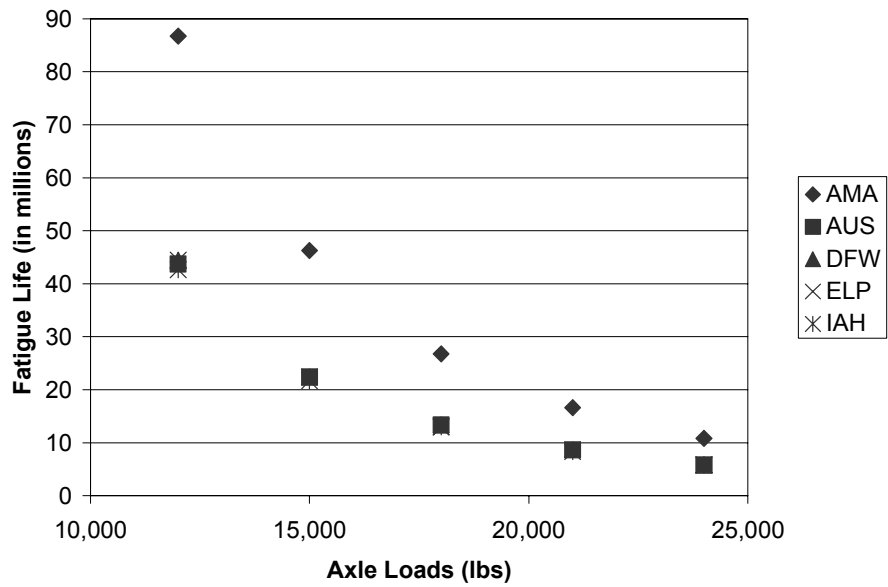


Figure 4.18: Fatigue Life of Structure 4 for Single Axle Loads

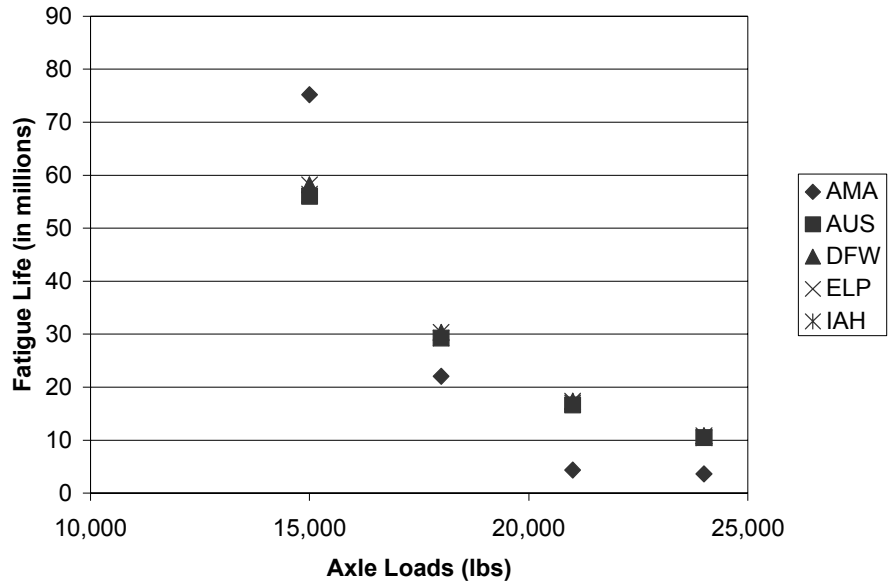


Figure 4.19: Fatigue Life of Structure 5 for Single Axle Loads

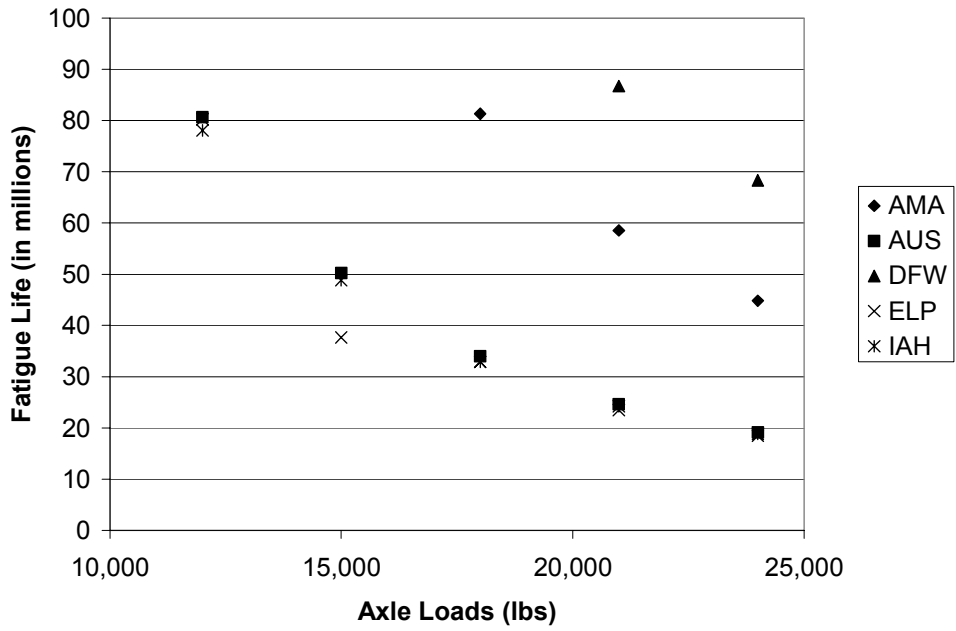


Figure 4.20: Fatigue Life of Structure 6 for Single Axle Loads

Fatigue life at the five locations in the case of tandem axle loads is given in Table 4.5.

Table 4.5: Fatigue Life for Tandem Axle Loads

Location	Structure	Tandem Axle Load (lbs.)				
		26,000	30,000	34,000	38,000	42,000
AMA	S1	75,542,100	56,746,900	44,457,800	33,253,000	27,108,400
	S2	41,090,600	29,448,300	22,599,800	17,121,100	14,039,300
	S3	3,614,450	3,253,010	2,530,120	2,168,670	2,168,670
	S4	37,228,900	24,216,800	16,265,000	11,566,300	8,674,690
	S5	83,493,900	35,783,100	10,120,500	3,975,900	3,614,450
	S6		86,746,900	58,192,700	39,397,500	28,192,700
AUS	S1	33,975,900	25,662,600	19,518,000	15,542,100	12,650,600
	S2	16,778,700	11,984,800	8,902,970	7,190,860	5,478,750
	S3	17,710,800	10,843,400	7,228,910	5,421,680	3,975,900
	S4	18,433,700	11,927,700	8,674,690	6,144,570	4,698,790
	S5	62,168,600	36,867,400	23,855,400	15,903,600	11,204,800
	S6	86,746,900	53,493,900	34,698,800	24,216,800	16,987,900
DFW	S1		74,457,700	59,999,900	49,518,000	41,204,800
	S2	34,927,000	24,654,400	18,833,200	14,724,100	11,642,300
	S3	18,433,700	11,566,300	7,590,350	5,421,680	3,975,900
	S4	19,156,600	12,289,100	8,674,690	6,144,570	4,698,790
	S5	66,144,500	39,397,500	25,301,200	16,626,500	11,927,700
	S6	86,746,900	56,385,500	36,867,400	25,301,200	18,072,300
ELP	S1	34,337,300	24,939,700	19,156,600	14,819,300	11,927,700
	S2	20,545,300	14,724,100	10,957,500	8,560,550	6,848,440
	S3	7,875,700	4,451,480	3,424,220	2,739,380	2,396,950
	S4	19,156,600	12,289,100	8,674,690	6,144,570	4,698,790
	S5	63,252,900	37,590,300	24,216,800	15,903,600	11,204,800
	S6	86,746,900	54,216,800	35,060,200	24,216,800	17,349,400
IAH	S1	32,530,100	24,216,800	19,156,600	15,180,700	13,012,000
	S2	15,409,000	10,615,100	7,875,700	6,163,590	4,793,910
	S3	7,875,700	4,793,910	3,424,220	2,739,380	2,396,950
	S4	18,072,300	11,566,300	8,313,240	6,144,570	4,698,790
	S5	66,144,500	39,397,500	25,301,200	16,626,500	11,927,700
	S6	85,301,100	51,686,700	33,614,400	23,493,900	16,626,500

Plots of the fatigue life under tandem axle loads at each location are shown in Figures 4.21 through 4.26 for structures 1 through 6, respectively. Results similar to those from single axles were observed from fatigue life under tandem axles. It is again observed that as the axle loads are increased from 26,000 lbs. to 42,000 lbs., the number of axle load repetitions required for the pavements to reach 10 percent fatigue cracking is reduced from 75,000,000 (AMA S1) to 2,000,000 (AMA S3), implying increased pavement deterioration.

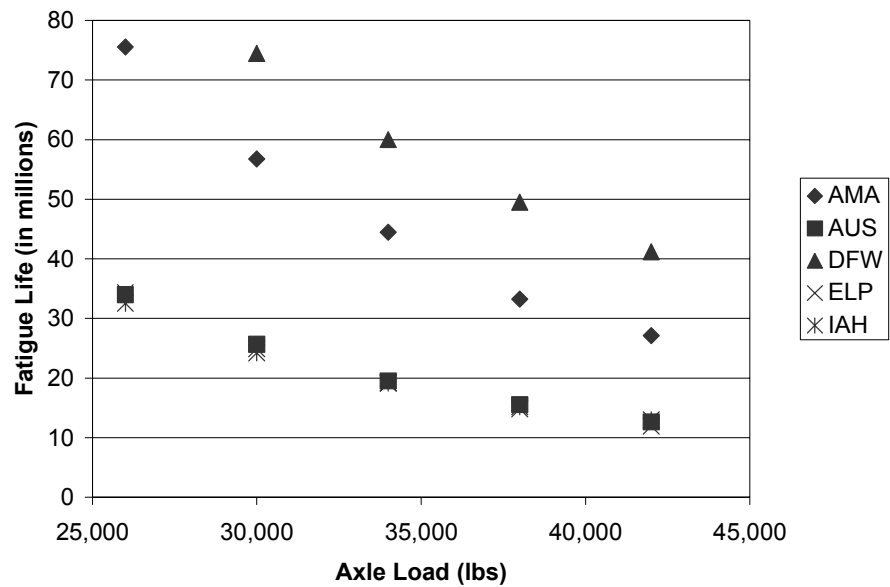


Figure 4.21: Fatigue Life of Structure 1 for Tandem Axle Loads

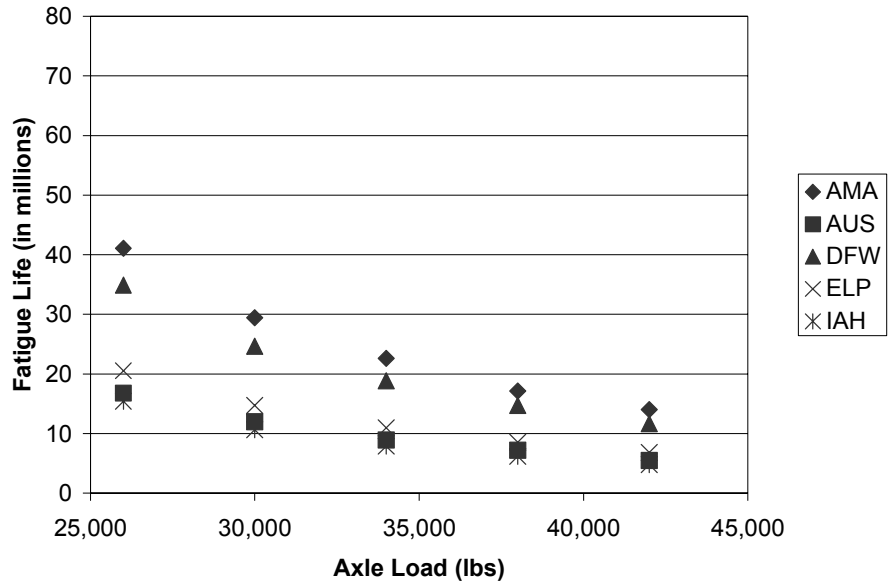


Figure 4.22: Fatigue Life of Structure 2 for Tandem Axle Loads

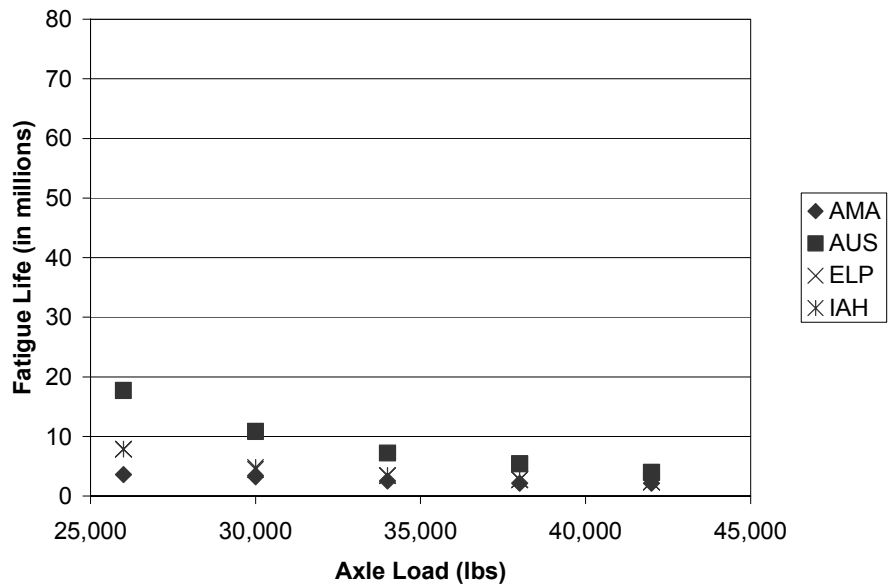


Figure 4.23: Fatigue Life of Structure 3 for Tandem Axle Loads

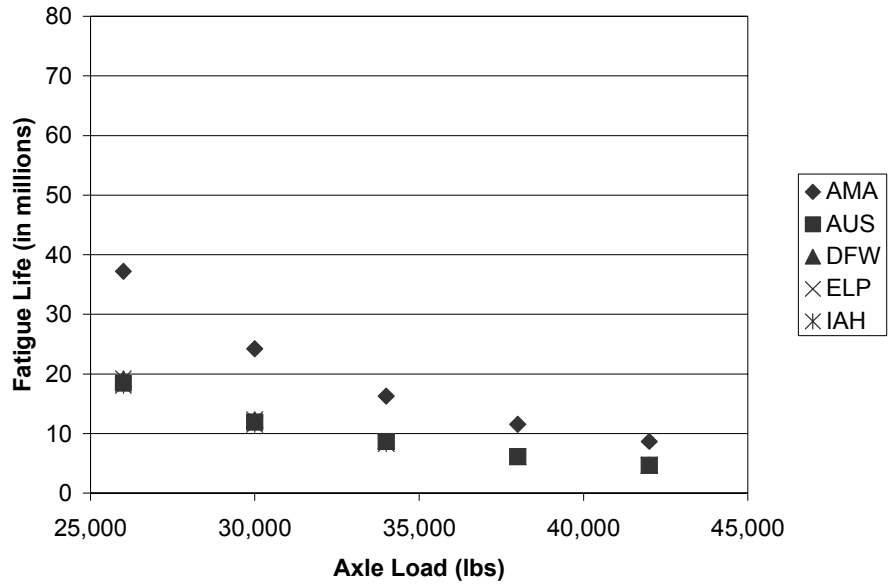


Figure 4.24: Fatigue Life of Structure 4 for Tandem Axle Loads

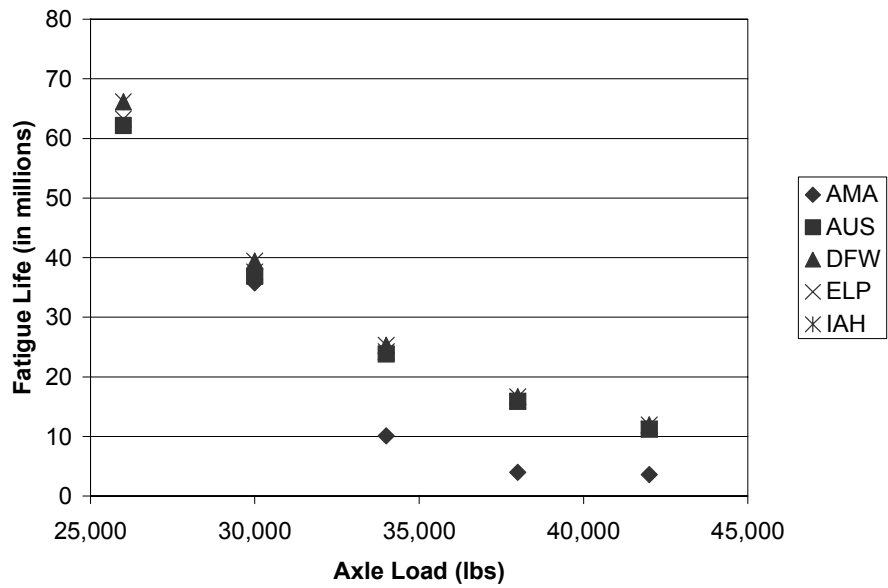


Figure 4.25: Fatigue Life of Structure 5 for Tandem Axle Loads

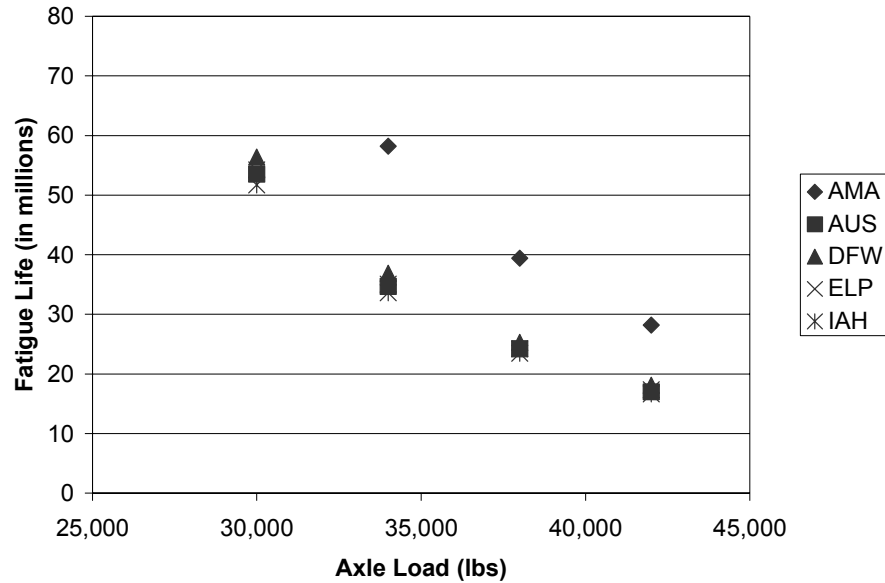


Figure 4.26: Fatigue Life of Structure 6 for Tandem Axle Loads

4.2 Equivalent Damage Factors (EDF)

Since the number of axle load repetitions needed to reach pavement failure vary for different conditions, it is important to compare the results of pavement life under different conditions, and to determine the effects of axle loads, axle types, SN, and environmental conditions on pavement performance. To compare pavement deterioration, the concept of EDF is used to analyze relative pavement life based on a standard load configuration. For the purpose of this research, the standard axle configuration consists of 18 kips single axle load. A standard load of 34 kips was used in the case of tandem axles, as 34 kips is the maximum allowable legal load limit in Texas. EDF is defined as the ratio of the number of repetitions for a standard load to the number of repetitions for a given load for the pavement to reach failure. Since failure can be defined in terms of various distresses such as surface rutting and fatigue cracking, several different EDF can be defined. The equation that defines EDF is shown in Equation 4.1.

$$\text{EDF} = \frac{N_{L_s}}{N_{L_x}} \quad (4.1)$$

Where,

N_{L_s} = axle repetitions under a standard axle load to reach failure

N_{L_x} = axle repetitions under any axle load to reach failure

L_s = standard axle load (18 kips for single axle and 34 kips for tandem axle)

L_x = load on one single axle or a set of tandem axles, in kips

Following are the results and analysis for rutting and fatigue cracking of the pavement structures.

4.2.1 Rutting

Using the results given in Tables 4.1 and 4.2, EDF values are tabulated in Tables 4.6 and 4.7. It can be observed that EDF values increase with the rise in axle loads, indicating that relative damage escalates with the increase in axle loads. Single axle load EDF values for all structures at all locations are shown in figures 4.27(a) and 4.27(b); values for tandem axle loads are shown in figures 4.28(a) and 4.28(b).

Table 4.6: EDF Values Using 18 kips Single Axle as the Standard Load for Pavements to Reach 0.5-inch Rutting

		Single Axle Load (lbs.)					Tandem Axle Load (lbs.)				
		12000	15000	18000	21000	24000	26000	30000	34000	38000	42000
AMA	S1	0.50	0.71	1.00	1.40	1.97	1.57	2.03	2.57	3.47	4.92
	S2	0.45	0.69	1.00	1.47	2.21	1.32	1.86	2.41	3.31	4.61
	S3	0.36	0.79	1.00	1.37	1.72	1.72	2.31	2.70	3.68	3.86
	S4	0.60	0.80	1.00	1.21	1.51	1.73	2.06	2.45	3.02	3.30
	S5	0.70	0.78	1.00	1.24	1.50	1.60	2.12	2.77	3.13	3.27
	S6	0.65	0.81	1.00	1.19	1.44	1.85	2.15	2.63	2.77	3.30
AUS	S1	0.48	0.70	1.00	1.37	1.75	1.47	1.70	2.43	2.80	4.31
	S2	0.43	0.74	1.00	1.32	1.96	1.29	1.80	2.14	3.46	4.09
	S3	0.75	0.92	1.00	1.26	1.33	1.42	1.91	2.20	3.38	3.67
	S4	0.58	0.73	1.00	1.24	1.33	1.49	1.74	1.79	2.44	2.65
	S5	0.73	0.76	1.00	1.03	1.13	1.52	1.67	2.69	2.92	3.18
	S6	0.66	0.77	1.00	1.22	1.48	1.58	1.97	2.03	2.15	2.96
DFW	S1	0.50	0.73	1.00	1.36	1.98	1.64	2.11	2.71	3.80	4.32
	S2	0.41	0.68	1.00	1.52	2.09	1.46	2.03	2.52	3.32	3.48
	S3	0.60	0.73	1.00	1.26	1.66	1.66	2.32	2.52	2.64	2.76
	S4	0.58	0.79	1.00	1.17	1.56	1.67	2.07	2.71	2.88	3.96
	S5	0.59	0.80	1.00	1.09	1.37	1.71	2.09	2.18	2.29	2.40
	S6	0.64	0.76	1.00	1.14	1.30	1.81	2.23	2.33	3.06	3.15
ELP	S1	0.45	0.71	1.00	1.36	1.94	1.36	1.94	2.73	3.16	5.00
	S2	0.40	0.66	1.00	1.41	2.18	1.37	2.00	2.29	3.69	4.36
	S3	0.57	0.78	1.00	1.31	1.84	2.00	2.19	2.42	3.83	4.18
	S4	0.62	0.82	1.00	1.27	1.67	1.78	2.35	3.33	3.64	3.81
	S5	0.59	0.78	1.00	1.29	1.57	1.71	1.89	3.00	3.27	3.60
	S6	0.63	0.78	1.00	1.19	1.38	1.80	2.31	2.59	3.61	3.77
IAH	S1	0.45	0.72	1.00	1.50	2.09	1.50	1.97	2.65	3.29	4.31
	S2	0.34	0.59	1.00	1.37	2.00	1.33	1.55	2.18	2.53	4.00
	S3	0.60	0.80	1.00	1.30	1.63	1.63	1.97	2.48	2.71	3.00
	S4	0.61	0.81	1.00	1.19	1.61	1.86	2.21	2.71	2.79	3.80
	S5	0.57	0.80	1.00	1.31	1.34	1.47	2.04	2.14	2.24	2.76
	S6	0.64	0.80	1.00	1.15	1.34	1.84	2.28	2.82	3.06	3.15

Table 4.7: EDF Values Using 34 kips Tandem Axle as the Standard Load for Pavements to Reach 0.5-inch Rutting

		Tandem Axle Load (lbs.)				
		26,000	30,000	34,000	38,000	42,000
AMA	S1	0.61	0.79	1.00	1.35	1.92
	S2	0.55	0.77	1.00	1.38	1.91
	S3	0.64	0.86	1.00	1.36	1.43
	S4	0.71	0.84	1.00	1.23	1.35
	S5	0.58	0.76	1.00	1.13	1.18
	S6	0.70	0.82	1.00	1.05	1.26
AUS	S1	0.61	0.70	1.00	1.15	1.77
	S2	0.60	0.84	1.00	1.62	1.91
	S3	0.65	0.87	1.00	1.54	1.67
	S4	0.83	0.97	1.00	1.36	1.48
	S5	0.57	0.62	1.00	1.08	1.18
	S6	0.78	0.97	1.00	1.06	1.46
DFW	S1	0.60	0.78	1.00	1.40	1.59
	S2	0.58	0.81	1.00	1.32	1.38
	S3	0.66	0.92	1.00	1.05	1.10
	S4	0.61	0.76	1.00	1.06	1.46
	S5	0.79	0.96	1.00	1.05	1.10
	S6	0.78	0.96	1.00	1.31	1.35
ELP	S1	0.50	0.71	1.00	1.16	1.83
	S2	0.60	0.87	1.00	1.62	1.91
	S3	0.83	0.90	1.00	1.58	1.73
	S4	0.53	0.71	1.00	1.09	1.14
	S5	0.57	0.63	1.00	1.09	1.20
	S6	0.70	0.89	1.00	1.39	1.45
IAH	S1	0.57	0.74	1.00	1.24	1.63
	S2	0.61	0.71	1.00	1.16	1.83
	S3	0.66	0.79	1.00	1.10	1.21
	S4	0.69	0.81	1.00	1.03	1.40
	S5	0.69	0.96	1.00	1.05	1.29
	S6	0.66	0.81	1.00	1.09	1.12

The EDF values in Tables 4.6 and 4.7 show that as the axle load is increased, the number of axle load repetitions required for the pavements to reach failure decreases. Hence, the EDF values increase as the axle loads also increase for a particular structure and location.

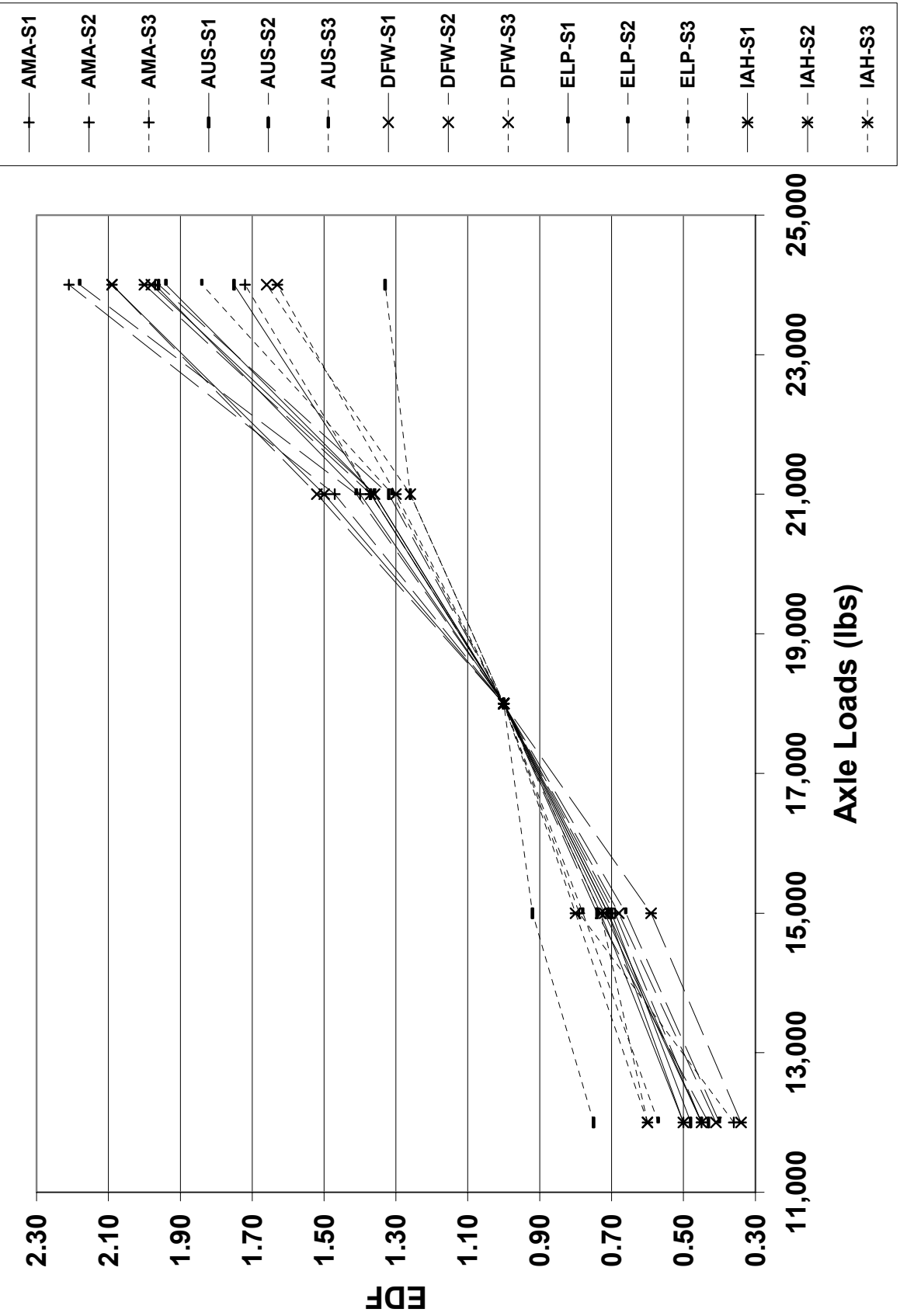


Figure 4.27 (a): EDF Values Using 18 kips Single Axle as the Standard Load for Pavements to Reach 0.5-inch Rutting

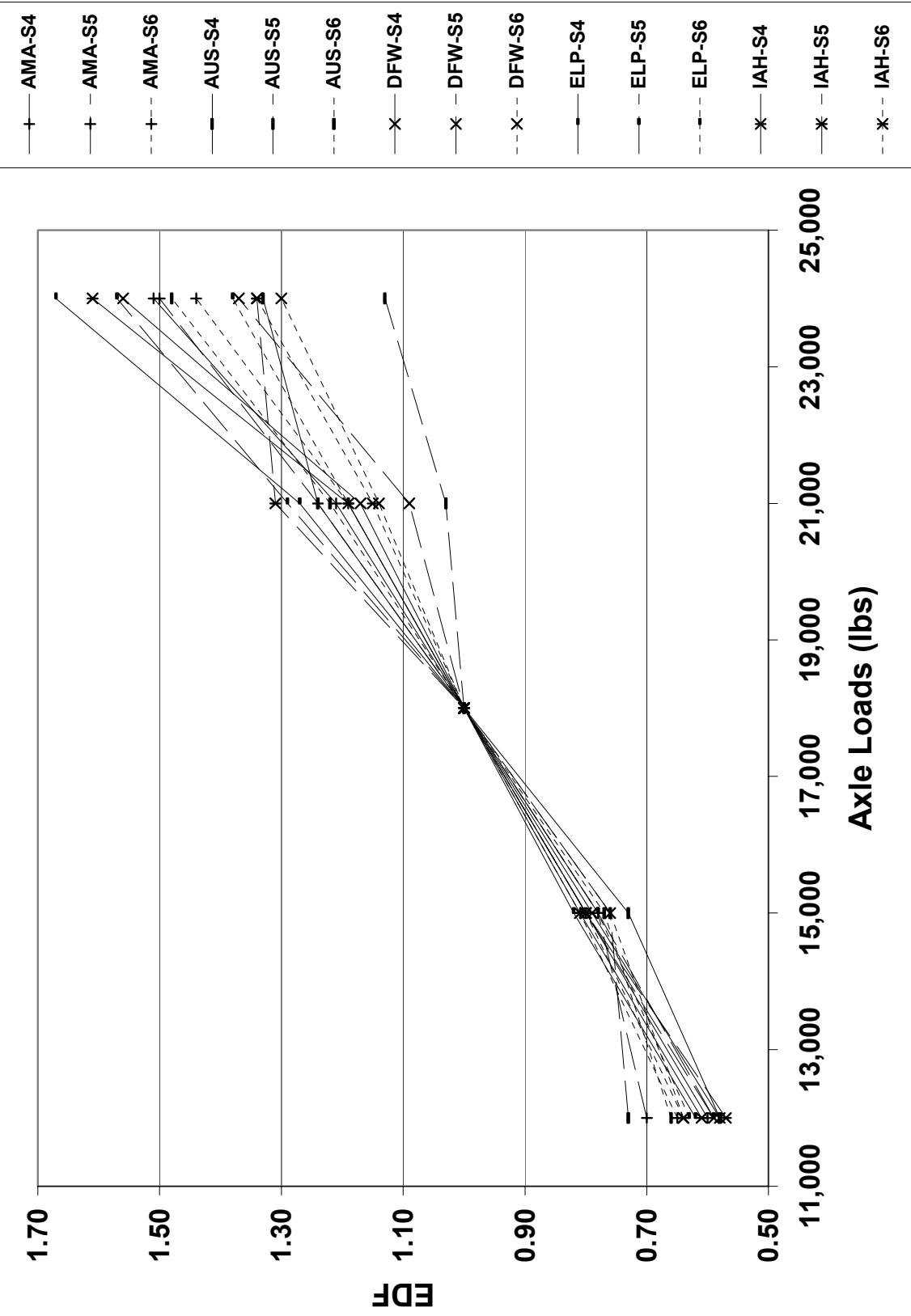


Figure 4.27 (b): EDF Values Using 18 kips Single Axle as the Standard Load for Pavements to Reach 0.5-inch Rutting

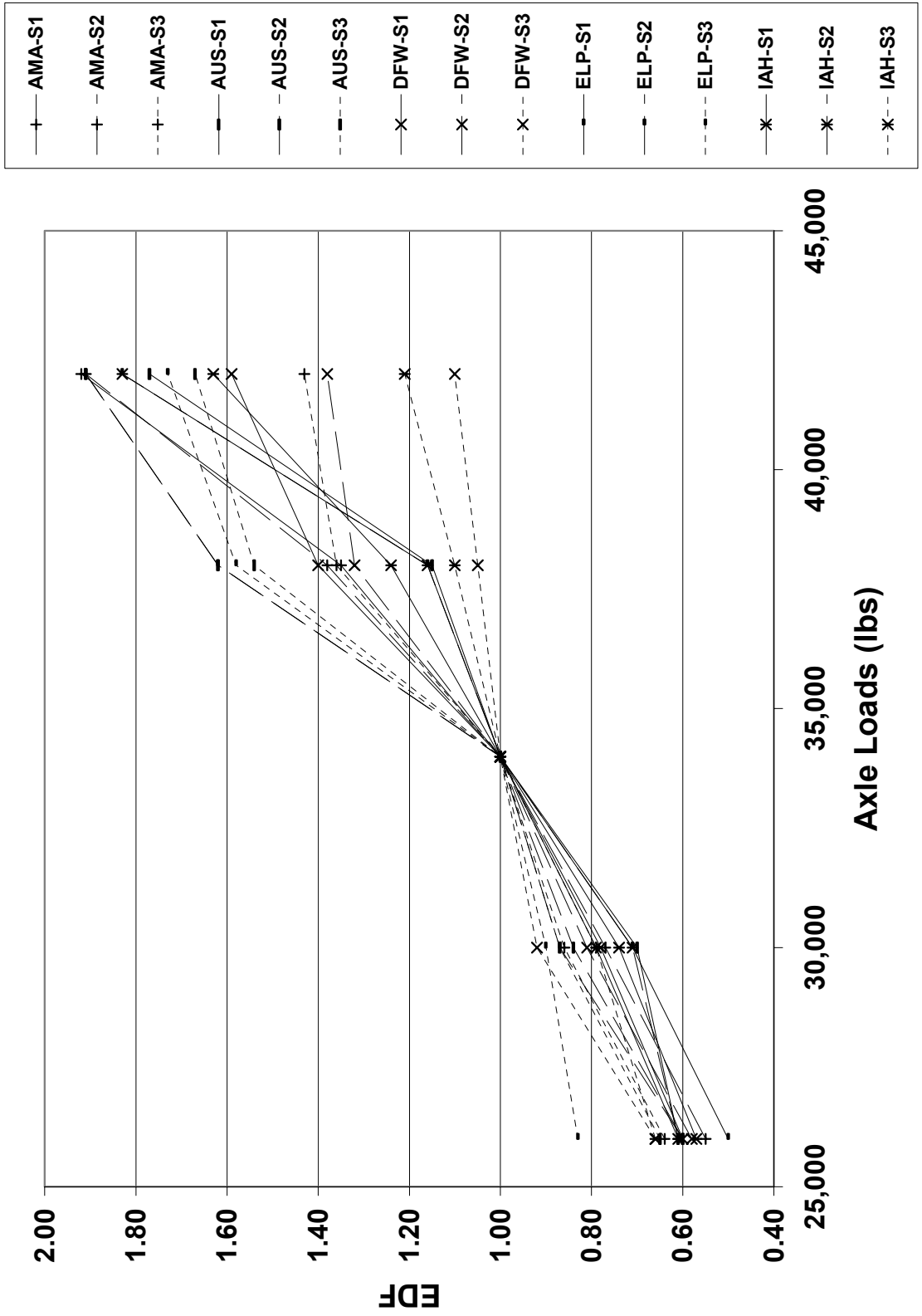


Figure 4.28 (a): EDF Values Using 34 kips Tandem Axle as the Standard Load for Pavements to Reach 0.5-inch Rutting

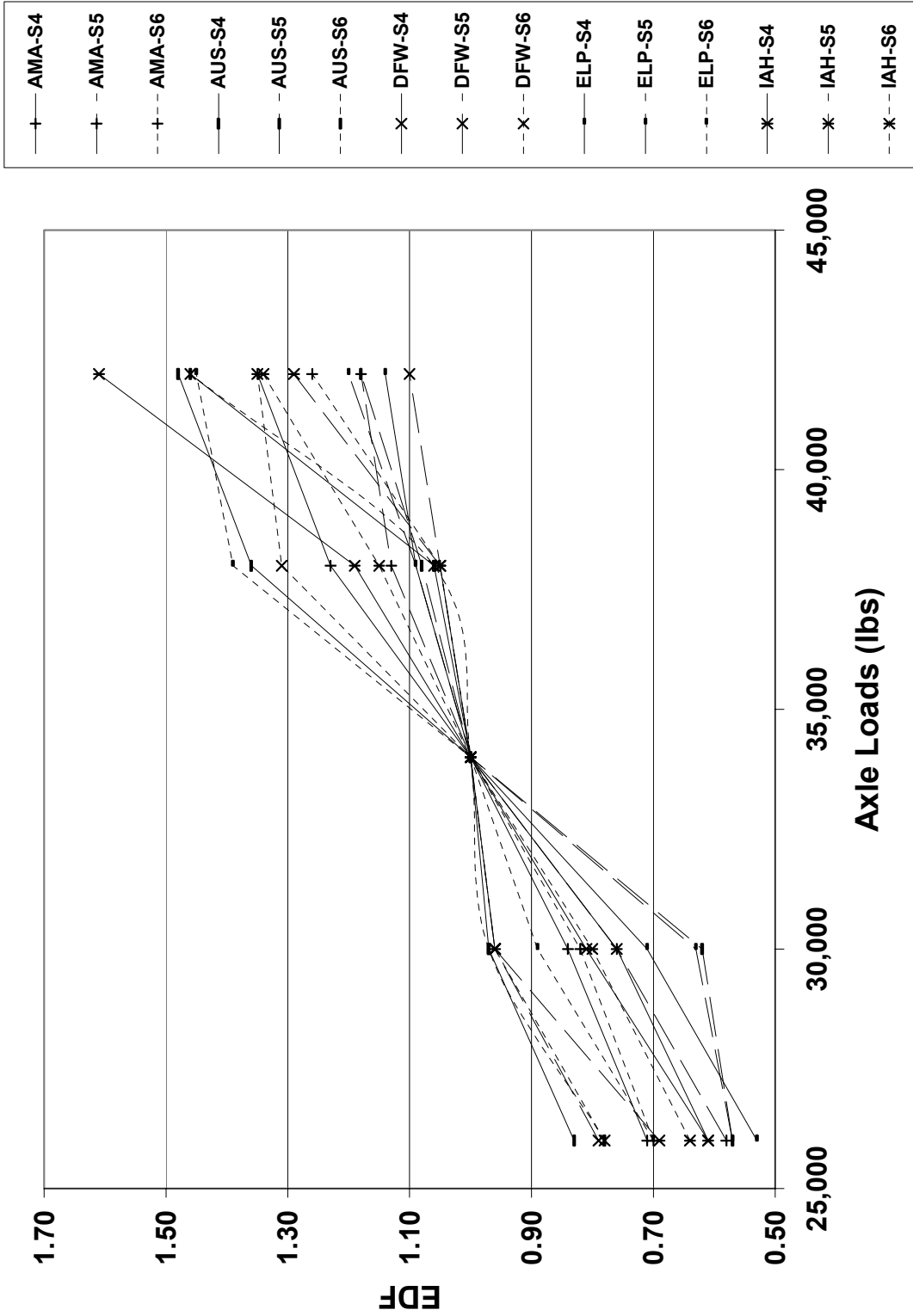


Figure 4.28 (b): EDF Values Using 34 kips Tandem Axle as the Standard Load for Pavements to Reach 0.5-inch Rutting

Figures 4.27(a), 4.27(b), 4.28(a), and 4.28(b) show that as the axle load increases, the EDF values increase at a higher rate, which implies that the increase in axle loads causes a more-than-proportional increase in pavement deterioration.

4.2.2 Fatigue Cracking

EDF values were also calculated based on fatigue performance using both 18 kips and 34 kips standard axle load, as shown in Tables 4.8 and 4.9 and plotted in figures 4.29(a), 4.29(b), 4.30(a) and 4.30(b).

It can be observed from Figures 4.29(a and b) and 4.30(a and b) that as axle load increases, EDF values increase at a higher proportion, which implies that the increase in axle loads causes a more-than-proportional increase in pavement deterioration. While the results of fatigue are compared with those of rutting, as the load increases, EDF value increases for both rutting and fatigue. However, the rate of increase of EDF value is higher for fatigue than for rutting. Hence, it can be said that the EDF slope is higher for fatigue than for rutting.

Table 4.8: EDF Under Varying Axle Loads–10 Percent Fatigue Cracking

		Single Axle Load (lbs.)					Tandem Axle Load (lbs.)				
		12000	15000	18000	21000	24000	26000	30000	34000	38000	42000
AMA	S1			1.00	1.39	1.81	1.08	1.43	1.83	2.45	3.00
	S2		0.67	1.00	1.42	1.90	0.98	1.37	1.79	2.36	2.88
	S3	0.12	0.82	1.00	1.29	1.50	0.90	1.00	1.29	1.50	1.50
	S4	0.31	0.58	1.00	1.61	2.47	0.72	1.10	1.64	2.31	3.08
	S5		0.29	1.00	5.08	6.10	0.26	0.62	2.18	5.55	6.10
	S6			1.00	1.70	2.71		0.88	1.31	1.94	2.71
AUS	S1	0.42	0.68	1.00	1.38	1.77	1.00	1.32	1.74	2.19	2.69
	S2	0.34	0.61	1.00	1.43	1.92	1.02	1.43	1.92	2.38	3.13
	S3	0.27	0.54	1.00	1.63	2.21	0.63	1.03	1.55	2.07	2.82
	S4	0.31	0.60	1.00	1.54	2.31	0.73	1.12	1.54	2.18	2.85
	S5		0.52	1.00	1.76	2.79	0.47	0.79	1.23	1.84	2.61
	S6		0.54	1.00	1.67	2.59	0.53	0.86	1.32	1.90	2.70
DFW	S1				0.00	0.00		0.00	0.00	0.00	0.00
	S2	0.43	0.66	1.00	1.43	1.91	1.01	1.43	1.87	2.40	3.03
	S3	0.27	0.55	1.00	1.68	2.46	0.63	1.00	1.52	2.13	2.91
	S4	0.30	0.60	1.00	1.54	2.31	0.70	1.09	1.54	2.18	2.85
	S5		0.52	1.00	1.75	2.80	0.46	0.77	1.20	1.83	2.55
	S6		0.54	1.00	1.67	2.60	0.54	0.83	1.27	1.86	2.60
ELP	S1	0.41	0.87	1.00	1.40	1.78	0.96	1.32	1.72	2.22	2.76
	S2	0.35	0.61	1.00	1.42	1.97	1.02	1.42	1.91	2.44	3.05
	S3	0.21	0.50	1.00	1.40	2.00	0.61	1.08	1.40	1.75	2.00
	S4	0.29	0.58	1.00	1.50	2.25	0.68	1.06	1.50	2.12	2.77
	S5		0.52	1.00	1.72	2.79	0.46	0.78	1.21	1.84	2.61
	S6		0.53	1.00	1.67	2.59	0.53	0.85	1.31	1.90	2.65
IAH	S1	0.42	0.67	1.00	1.36	1.75	1.01	1.36	1.72	2.17	2.53
	S2	0.33	0.62	1.00	1.47	2.00	0.98	1.42	1.91	2.44	3.14
	S3	0.23	5.36	1.00	1.50	1.87	0.65	1.07	1.50	1.87	2.14
	S4	0.31	0.60	1.00	1.57	2.25	0.72	1.12	1.57	2.12	2.77
	S5		0.52	1.00	1.75	2.80	0.46	0.77	1.20	1.83	2.55
	S6		0.53	1.00	1.67	2.60	0.52	0.85	1.31	1.88	2.65

Table 4.9: EDF Under Varying Axle Loads–10 Percent Fatigue Cracking

Location	Structure	Tandem Axle Load (lbs.)				
		26000	30000	34000	38000	42000
AMA	S1	0.59	0.78	1.00	1.34	1.64
	S2	0.55	0.77	1.00	1.32	1.61
	S3	0.70	0.78	1.00	1.17	1.17
	S4	0.44	0.67	1.00	1.41	1.87
	S5	0.12	0.28	1.00	2.55	2.80
	S6		0.67	1.00	1.48	2.06
AUS	S1	0.57	0.76	1.00	1.26	1.54
	S2	0.53	0.74	1.00	1.24	1.63
	S3	0.41	0.67	1.00	1.33	1.82
	S4	0.47	0.73	1.00	1.41	1.85
	S5	0.38	0.65	1.00	1.50	2.13
	S6	0.40	0.65	1.00	1.43	2.04
DFW	S1		0.81	1.00	1.21	1.46
	S2	0.54	0.76	1.00	1.28	1.62
	S3	0.41	0.66	1.00	1.40	1.91
	S4	0.45	0.71	1.00	1.41	1.85
	S5	0.38	0.64	1.00	1.52	2.12
	S6	0.42	0.65	1.00	1.46	2.04
ELP	S1	0.56	0.77	1.00	1.29	1.61
	S2	0.53	0.74	1.00	1.28	1.60
	S3	0.43	0.77	1.00	1.25	1.43
	S4	0.45	0.71	1.00	1.41	1.85
	S5	0.38	0.64	1.00	1.52	2.16
	S6	0.40	0.65	1.00	1.45	2.02
IAH	S1	0.59	0.79	1.00	1.26	1.47
	S2	0.51	0.74	1.00	1.28	1.64
	S3	0.43	0.71	1.00	1.25	1.43
	S4	0.46	0.72	1.00	1.35	1.77
	S5	0.38	0.64	1.00	1.52	2.12
	S6	0.39	0.65	1.00	1.43	2.02

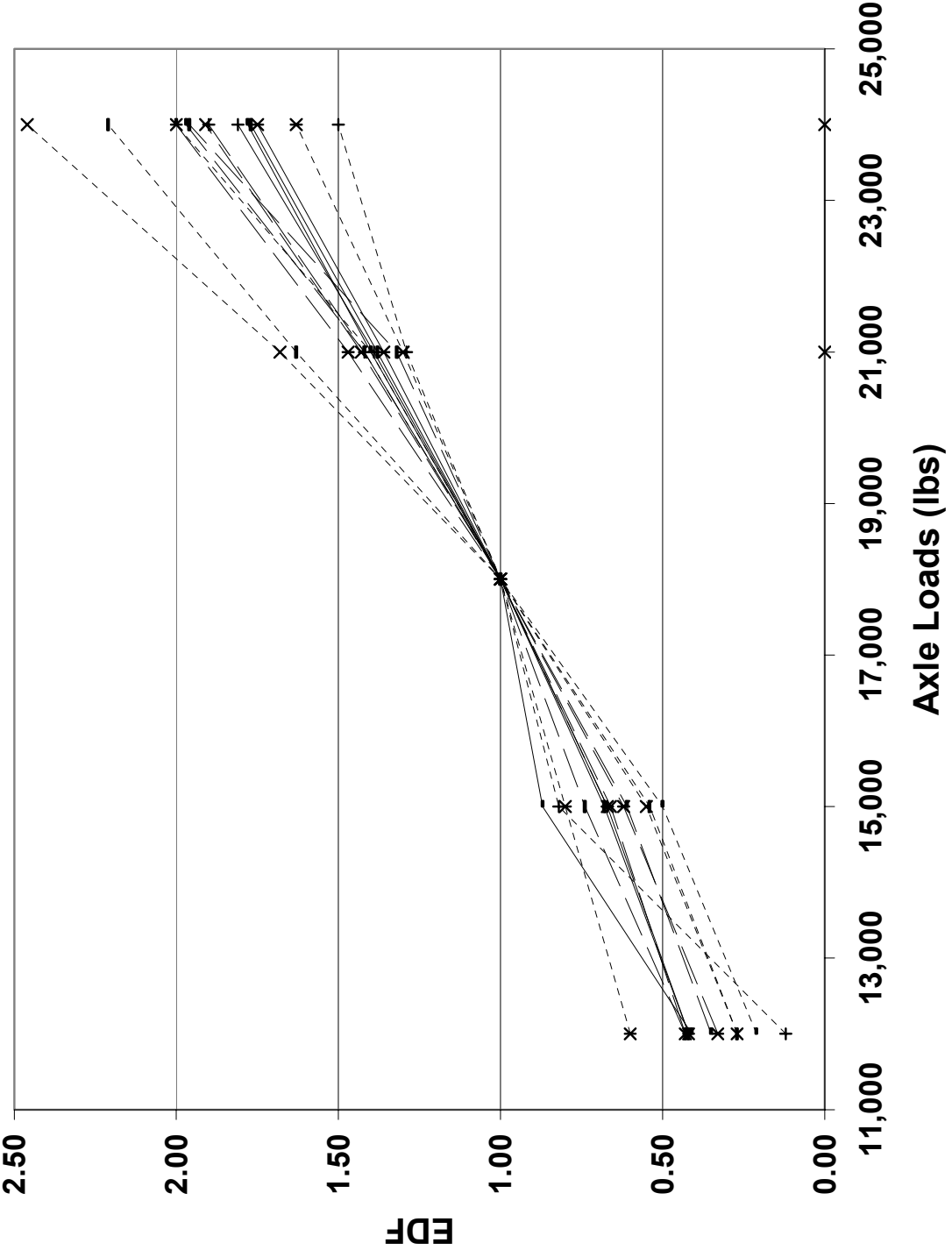
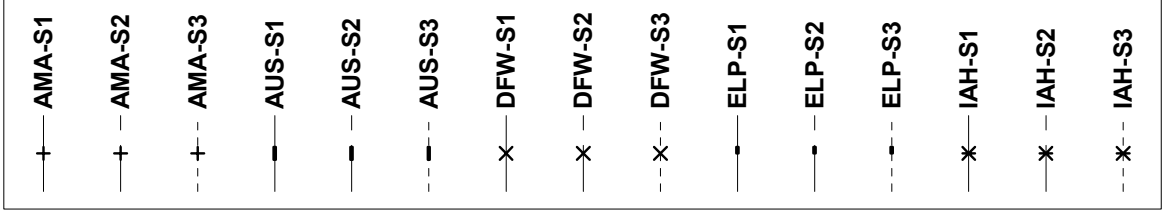


Figure 4.29 (a): EDF Values Using 18 kips Single Axle as the Standard Load for Fatigue Cracking

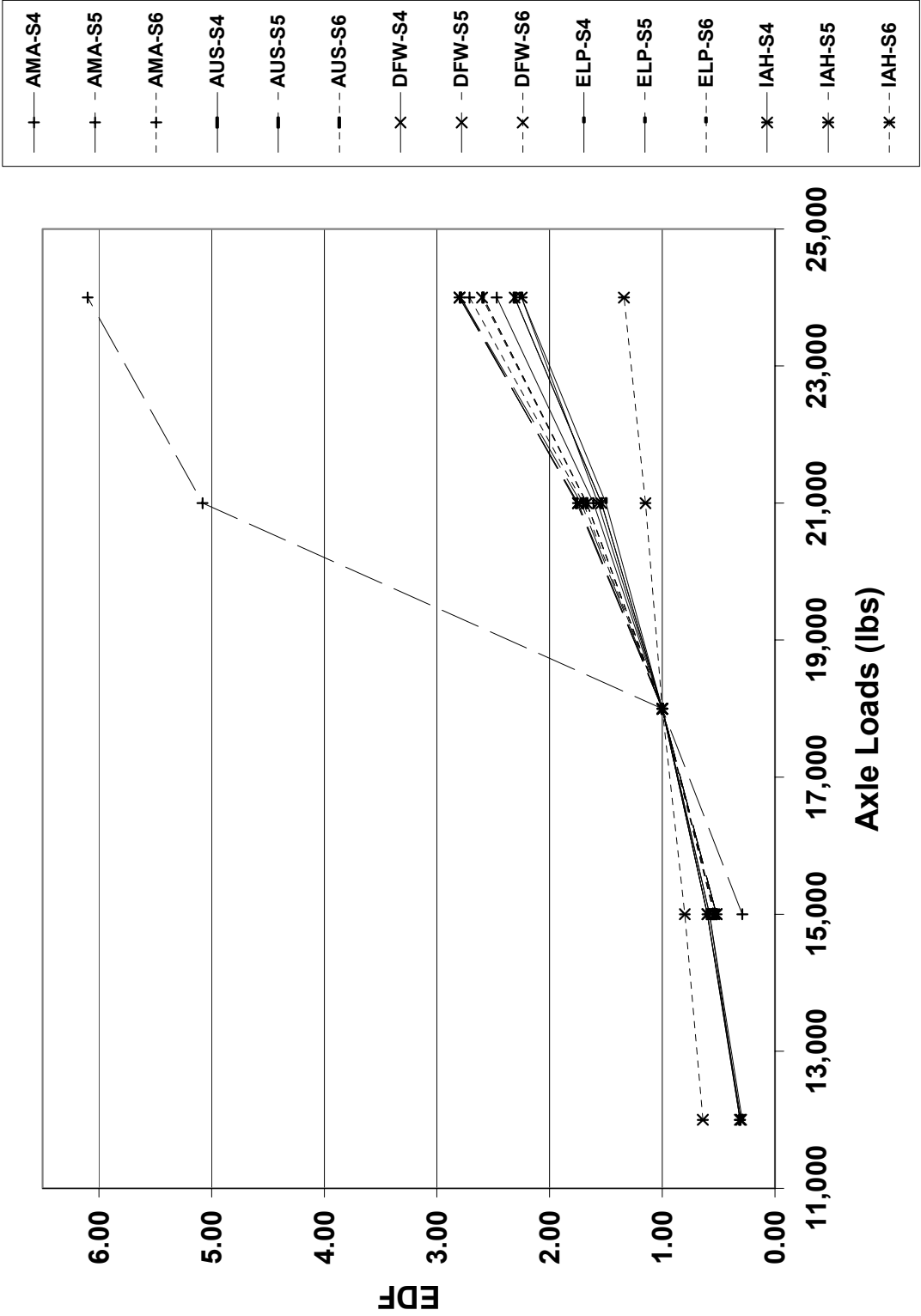


Figure 4.29 (b): EDF Values Using 18 kips Single Axle as the Standard Load for Fatigue Cracking

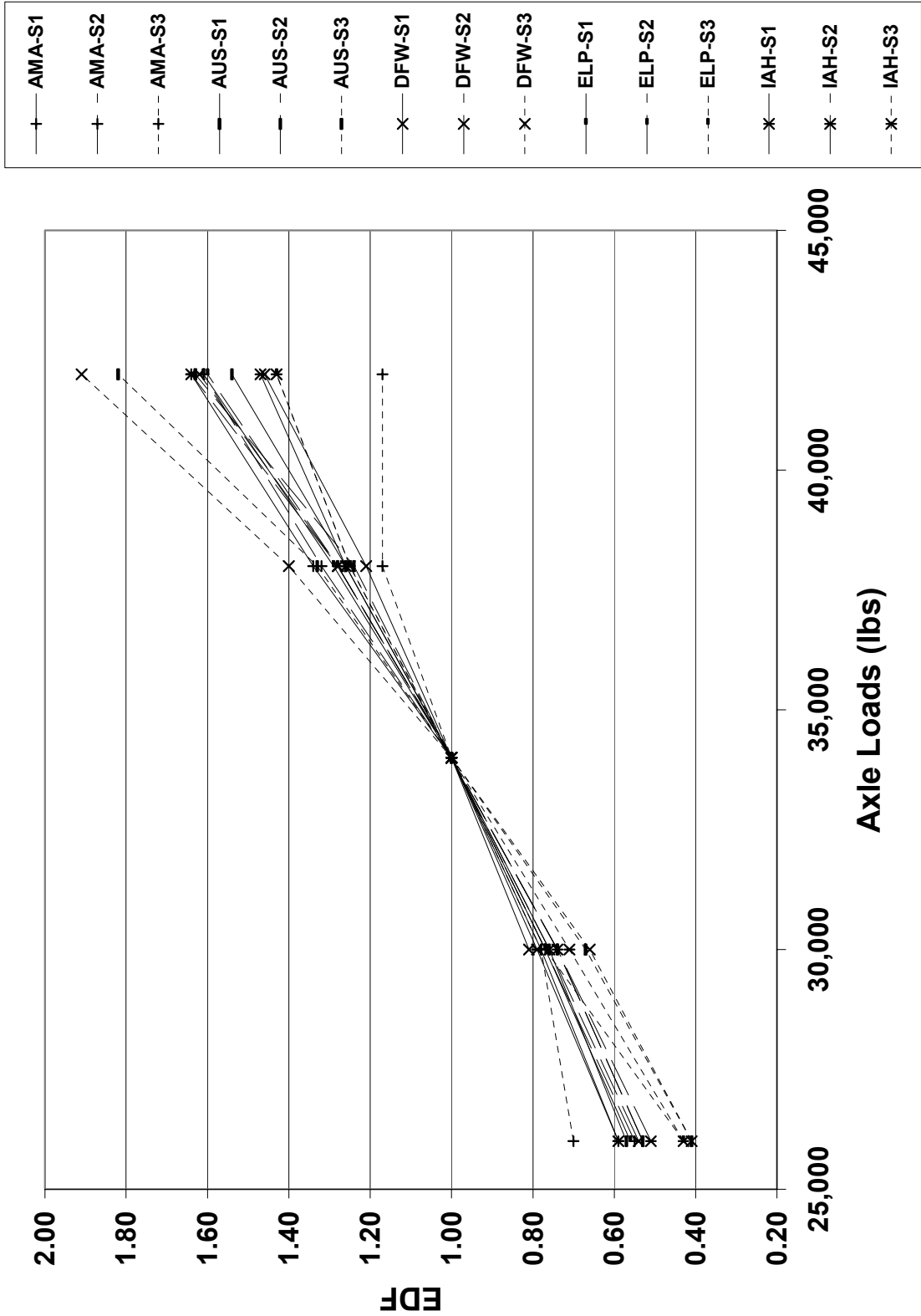


Figure 4.30 (a): EDF Values Using 34 kips Tandem Axle as the Standard Load for Fatigue Cracking

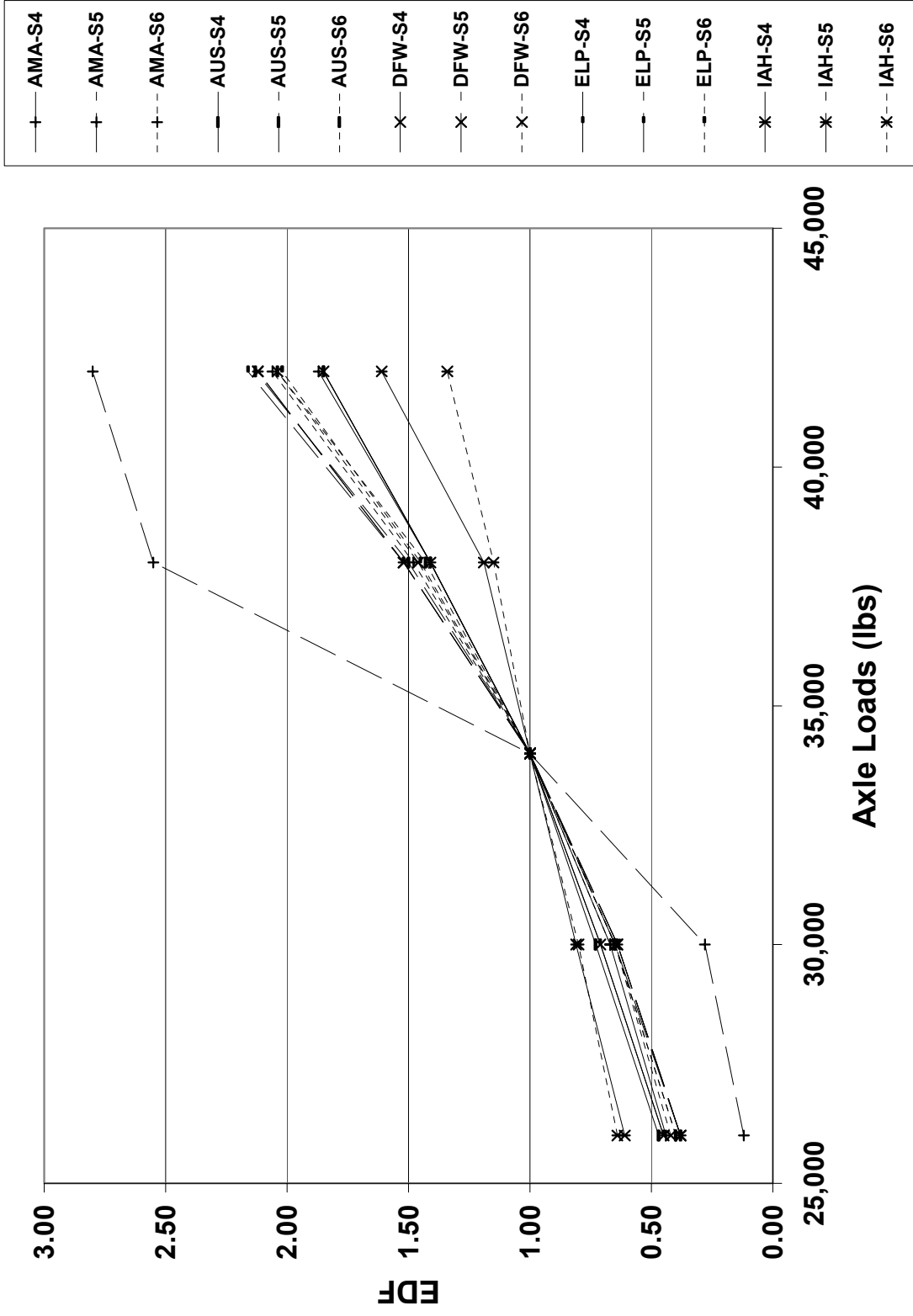


Figure 4.30 (b): EDF Values Using 34 kips Tandem Axle as the Standard Load for Fatigue Cracking

CHAPTER 5. REGRESSION ANALYSIS AND APPLICATIONS

5.1 Regression Analysis

Regression analyses were conducted to develop equations for estimating EDF. Linear regression was carried out using variable transformations such as linear, power, and exponential in order to obtain the best model. The equations estimate EDF as a function of relative axle load ($L/18,000$, where L is the load in lbs.), SN, location, and axle type. Locations are used as categorical data, and Houston was selected as the base location with four dummy variables for Amarillo, Austin, Dallas/Ft. Worth and El Paso. Axle type (single and tandem) was also used as categorical data, with single axle being the base type and tandem the dummy variable. The resulting models are discussed in the following sections.

5.1.1 *Fatigue Cracking*

Based on analysis of various linear regression transformations, the logarithmic transformation was selected to estimate fatigue-based EDF. The initial model is represented by Model 5.1 (Table 5.1) and its corresponding equation is shown in Equation 5.1. In order to determine the statistical significance of the variables, t-statistic was used. Although initially the plan was to eliminate the variables for which the t-statistic value was less than 1.96, it was observed that the model had t-statistic values lower than 1.96 for variables that should have a significant effect on performance. This development could be attributed to the relatively small sample size in relation to the number of variables considered. Based on this consideration, variables considered relevant were included in the final model despite their low t-statistics. Only those variables with very low t-statistics were removed.

From Model 5.1, it was observed that the DFW term had a very low t-statistic value of 0.02. Hence, Model 5.2 was created by eliminating the DFW term. Model 5.3 was created by eliminating the ELP term from Model 5.2 since ELP had the lowest t-statistic value of 0.31. The t-statistic value for the tandem term in Model 5.3 was low (0.61), hence Model 5.4 was created

by eliminating the tandem term. The remaining terms for Model 5.4 had t-statistic values greater than 1.1; therefore Model 5.4 was selected as the final model (see Equation 5.2).

The relative load and SN terms in Model 5.4 had a statistically significant impact on the model, as the t-statistic values for these terms were found to be greater than 1.1. AUS and AMA were the only statistically significant location terms, with t-statistic values greater than 1.1. The model statistics are given in Table 5.1.

Table 5.1: Regression Models for Fatigue-based EDF

MODEL	Initial Model 5.1		Intermediate Model 5.2		Intermediate Model 5.3		Final Model 5.4	
	Coeff.	t-stat	Coeff.	t-stat	Coeff.	t-stat	Coeff.	t-stat
ln(L/18000d)	0.82	3.98	0.82	4.1	0.84	4.34	0.82	4.31
ln(L/18000d).SN	0.56	11.01	0.56	11.07	0.56	11.09	0.56	11.09
ln(L/18000d).AMA	0.18	1.31	0.18	1.51	0.17	1.49	0.17	1.51
ln(L/18000d).AUS	0.15	1.06	0.16	1.2	0.14	1.17	0.14	1.13
ln(L/18000d).DFW	-0.002	-0.02	-	-	-	-	-	-
ln(L/18000d).ELP	0.04	0.26	0.04	0.31	-	-	-	-
ln(L/18000d).Tandem	-0.06	-0.61	-0.06	-0.61	-0.06	-0.61	-	-
No. of Observations	276		276		276		276	
Adjusted R ²	0.94		0.94		0.94		0.94	

$$\ln(EDF_{fat}) = \left\{ \ln(L/18,000 * d) \right\} \left\{ \begin{array}{l} 0.82 + 0.56(SN) + 0.18(AMA) + 0.15(AUS) \\ - 0.002(DFW) + 0.04(ELP) - 0.06(Tandem) \end{array} \right\}$$

(5.1)

$$\text{Adjusted } R^2 = 0.94$$

$$\ln(EDF_{fat}) = \{\ln(L/18,000 * d)\} \{0.82 + 0.56(SN) + 0.17(AMA) + 0.14(AUS)\} \quad (5.2)$$

Adjusted $R^2 = 0.94$

Where,

$$d = \begin{cases} 1.00 & \text{for single axle} \\ 34,000 / 18,000 = 1.89 & \text{for tandem axle} \end{cases}$$

In terms of fatigue, it is observed from the final regression model that pavements in Austin and Amarillo exhibit similar behavior in terms of EDF. The remaining locations — Houston, Dallas and El Paso — are expected to act in similar fashion while predicting fatigue-based EDF. It is noted from the slope parameters of the term representing SN that fatigue-based EDF increases as SN increases.

5.1.2 Rutting

EDF for rutting was best represented using a logarithmic transformation. The initial model comprising all the terms is given as Model 5.5 (see Equation 5.3). As in the case of fatigue-based EDF, t-statistic was used to analyze the statistical significance of the variables in the case of rutting-based EDF. It was observed from the initial model that the t-statistic value was less than 1.1 for the AMA term (0.88); therefore it was decided to eliminate the AMA term from the model, creating Model 5.6 as the final model. Model 5.6 is represented as Equation 5.4.

It was noted that the behavior of EDF for pavements in Amarillo is not significantly different from pavements in Houston. However, EDF of pavements in Austin, Dallas, and El Paso differ from EDF of pavements in Houston. The other variables — SN, axle type, and relative load — were seen to have a statistically significant impact on the EDF model. The regression models for this analysis are shown in Table 5.2.

Table 5.2: Regression Models for Rutting-based EDF

MODEL	Initial Model 5.5		Final Model 5.6	
Variable Name	Coeff.	t-stat	Coeff.	t-stat
ln(L/18000d)	2.99	23.26	3.03	25.22
ln(L/18000d).SN	-0.38	-12.9	-0.38	-12.91
ln(L/18000d).AMA	0.08	0.88	-	-
ln(L/18000d).AUS	-0.15	-1.6	-0.19	-2.36
ln(L/18000d).DFW	-0.11	-1.17	-0.15	-1.86
ln(L/18000d).ELP	0.13	1.42	0.09	1.13
ln(L/18000d).Tandem	0.13	2.12	0.13	2.13
No. of Observations	300		300	
Adjusted R ²	0.91		0.91	

$$\ln(EDF_{rut}) = \{\ln(L/18000 * d)\} \left\{ \begin{array}{l} 2.99 - 0.38(SN) + 0.08(AMA) - 0.15(AUS) \\ - 0.11(DFW) + 0.13(ELP) + 0.13(Tandem) \end{array} \right\} \quad (5.3)$$

$$\text{Adjusted } R^2 = 0.91$$

$$\ln(EDF_{rut}) = \{\ln(L/18000 * d)\} \left\{ \begin{array}{l} 3.03 - 0.38(SN) - 0.19(AUS) - 0.15(DFW) \\ + 0.09(ELP) + 0.13(Tandem) \end{array} \right\} \quad (5.4)$$

$$\text{Adjusted } R^2 = 0.91$$

Where,

$$d = \begin{cases} 1 & \text{for single axle} \\ 34,000/18,000 = 1.89 & \text{for tandem axle} \end{cases}$$

It can be observed from Model 5.6 that for a given load and axle type, Austin and Dallas have lower EDF values compared to the other locations.

Another interesting observation in the case of rutting-based EDF is that the axle type impacts EDF after applying load corrections. The positive slope of the tandem axle term indicates that for tandem axles, the rutting-based EDF value is greater than that for single axles.

It can be seen from Equations 5.2 and 5.4 that the slope of the relative axle load term has a physical meaning representing the average sensitivity of the analyzed pavement structures to load increases. This is equivalent to the exponent of the so-called power law, which states that pavement deterioration is a function of the fourth power of axle load, and hence the increase in pavement deterioration is more than proportional to the increase in axle loads. Equation 5.5 was developed based on the analysis of the results of the AASHO Road Test.

$$LEF = \left(\frac{L}{18,000} \right)^4 \quad (5.5)$$

The final models for the two cases of fatigue-based and rutting-based EDF are given in Table 5.3. As the SN increases, fatigue-based EDF increases, whereas rutting-based EDF decreases. Another interesting observation is that for a given load and axle type, in the case of fatigue-based EDF, Austin and Amarillo have higher EDF values as compared to other locations. Whereas, in the case of rutting-based EDF, Austin and Dallas have lower EDF values compared to the other locations.

Table 5.3: Final Regression Models for Fatigue- and Rutting-based EDF

MODEL	Fatigue		Rutting	
	Final Model 5.4		Final Model 5.6	
Variable Name	Coeff.	t-stat	Coeff.	t-stat
ln(L/18000d)	0.82	4.31	3.03	25.22
ln(L/18000d).SN	0.56	11.09	-0.38	-12.91
ln(L/18000d).AMA	0.17	1.51	-	-
ln(L/18000d).AUS	0.14	1.13	-0.19	-2.36
ln(L/18000d).DFW	-	-	-0.15	-1.86
ln(L/18000d).ELP	-	-	0.09	1.13
ln(L/18000d).Tandem	-	-	0.13	2.13
No. of Observations	276		300	
Adjusted R ²	0.94		0.91	

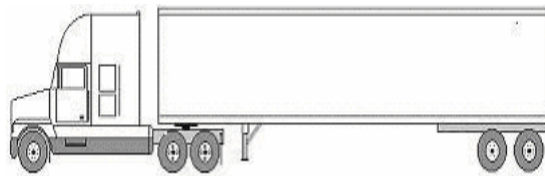
5.2 Case Study

In order to apply the results of this research to a different set of conditions, a pavement structure which lies between structure 2 (SN = 3.02) and structure 3 (SN = 3.48) was considered. The properties of this sample structure are shown in Table 5.4.

Table 5.4: Structural Properties of the Sample Structure

Structure	Layer	Material	Thickness (in.)	Modulus (psi)
Sample	Surface	Dense Asphalt	3	
	Base	A-1-b	7.5	75,000
	Subbase	A-2-4	8	45,000
	Subgrade	A-6	Semi-Infinite	8,000

The SN of this sample pavement was calculated as 3.25. This structure is assumed to be in Waco (TX), which is located midway between Austin and Dallas/Forth Worth. In order to estimate the pavement deterioration of this test structure, all traffic was assumed to consist of Class 9-type vehicles loaded under three different scenarios. The first scenario corresponds to a load of 58,000 lbs. The second scenario corresponds to a load of 80,000 lbs., and the third scenario represents vehicles that are 20 percent in excess of 80,000 lbs. The three load scenarios are represented in Figure 5.1.



Scenario	Single	Tandem	Tandem	Total
1	10	24	24	58
2	12	34	34	80
3	16	40	40	96

Figure 5.1: Axle Loads (kips) for a Class 9 Vehicle Used in the Case Study

The fatigue- and rutting-based EDF values for single and tandem axles and the total EDF ($EDF_{total} = EDF_{single} + 2 * EDF_{tandem}$) values for Class 9 vehicles in Austin for the three scenarios are obtained using Equations 5.2 and 5.4 and are given in Table 5.5. The values for Dallas are shown in Table 5.6. The EDF values for Austin and Dallas are linearly interpolated to get the estimated value of EDF for rutting and fatigue in Waco. The estimated EDF values for Waco are given in Table 5.7.

Table 5.5: Estimated EDF Values for Austin

Scenario	Fatigue EDF			Rutting EDF		
	Single	Tandem	EDF_{fat}	Single	Tandem	EDF_{rut}
1	0.20	0.38	0.96	0.39	0.55	1.49
2	0.33	1.00	2.33	0.52	1.00	2.52
3	0.54	1.66	3.86	0.83	1.33	3.49

Table 5.6: Estimated EDF Values for Dallas

Scenario	Fatigue EDF			Rutting EDF		
	Single	Tandem	EDF_{fat}	Single	Tandem	EDF_{rut}
1	0.21	0.40	1.01	0.38	0.54	1.46
2	0.35	1.00	2.35	0.51	1.00	2.51
3	0.56	1.61	3.78	0.82	1.33	3.48

Table 5.7: Estimated EDF Values for Waco

Scenario	EDF_{fat}	EDF_{rut}
1	0.99	1.48
2	2.34	2.52
3	3.82	3.49

Next, the fatigue life under a single axle 18 kips load for Waco is estimated by linearly interpolating the results of fatigue for Austin and Dallas, discussed in Chapter 4, which was found to be 18,885,808. Similarly, the rutting life for Waco is estimated to be 2,862,648. These fatigue and rutting lives are then converted to numbers of trucks required for failure using the EDF values given in Table 5.7.

The results of the estimated fatigue and rutting lives are then compared with those obtained by running the full simulation using the Design Guide. The Design Guide is simulated for Waco for the three load scenarios given in Figure 5.1. The failure criterion was based on 0.5-inch rutting and 10 percent fatigue cracking. The actual fatigue and rutting lives (in terms of numbers of trucks) obtained by running the full simulation and the estimated values are given in Table 5.8.

Table 5.8: Estimated vs. Actual Fatigue and Rutting Lives for Waco

Scenario	Fatigue		Rutting	
	Estimated	Design Guide	Estimated	Design Guide
1	19,076,574	19,860,500	1,934,222	1,814,930
2	8,030,096	6,506,020	1,135,971	908,141
3	4,918,959	4,109,060	820,243	657,463

Comparing the results of the estimated lives with those obtained using the Design Guide, fatigue error rates of 4 percent, 19 percent and 16 percent for the three scenarios, respectively, is obtained. A similar comparison of rutting results gives error rates of 6 percent, 20 percent, and 20 percent for the three scenarios, respectively. It is observed that as the load is increased from the first scenario to the second scenario (38 percent load increase), fatigue damage increases by 58 percent, while rutting damage increases by 41 percent. If the load is increased from the second scenario to the third (20 percent load increase), fatigue damage increases by 39 percent and rutting damage increases by 28 percent indicating that the increase in pavement failure is more than proportional to the increase in axle loads.

CHAPTER 6. CONCLUSIONS AND RECOMMENDATIONS

6.1 Conclusions

The recently developed mechanistic-empirical-based Design Guide was used in this research for the evaluation of pavement performance and the determination of EDF. The four major variables that were considered in this research study are:

1. pavement structural capacity (expressed in terms of the SN),
2. environmental conditions (five locations representative of the most typical Texas conditions were investigated),
3. axle loads (single and tandem axles), and
4. rutting and fatigue-cracking performance.

The failure criterion of the pavements in terms of surface rutting was 0.5 inch and 10 percent in terms of fatigue cracking. When compared to the empirical design based on AASHTO 1993, the mechanistic-based analysis estimates longer pavement lives for structures 1 and 2 and a similar estimate for structure 3. On the other hand, for structures 4, 5 and 6, the mechanistic-based analysis estimates longer pavement lives in terms of fatigue, and shorter pavement lives in terms of rutting compared to the empirical-based analysis. However, the failure criterion in AASHTO 1993 is based on riding quality in terms of PSI. Expected life as a function of the SN is sensitive when applying the empirical method, but markedly less sensitive when the mechanistic approach is used.

Based on the performance analyses, it was observed that Amarillo had the slowest pavement deterioration compared to the other locations that were chosen for this research project. The pace of deterioration was attributed to the colder weather prevailing in Amarillo. On the other hand, the fastest pavement deterioration was observed in Austin and El Paso, which could be due to their warmer climate.

The effect of using different axle loads for both single and tandem axles was also investigated as part of this research study. It was observed that as the axle load increased, pavement reached failure at a faster rate, requiring a lower number of repetitions to reach failure. It was also observed that as the axle load increased, the fatigue-based EDF increased at a much faster rate compared to rutting-based EDF. In all instances, deterioration occurred more slowly in Amarillo than the other locations.

EDF is the analysis of relative pavement life based on a standard axle load. The standard axle load chosen was 18,000 lbs. for single axle loads and 34,000 lbs. for tandem axle loads.

Regression analysis enabled the formulation of simple equations for directly estimating EDF. Variables such as axle loads, SN, and locations were considered, but only axle loads had a statistically significant impact on EDF. From these equations, it was concluded that fatigue-based EDF increased at a faster rate compared to rutting-based EDF when the axle load increased. This result was due to the fact that the SN term had a positive fatigue slope and a negative rutting slope.

Another observation was that as the SN increased to a particular value, which is the critical value of the SN, fatigue life decreased. As the SN was further increased, fatigue life increased. This critical value of the SN was observed to be between 3 and 4.

In order to see the application of these equations and to be able to compare the results of the estimated EDF values with those obtained by using the Design Guide, a case study was conducted. The error between the estimated and the actual values was low for both fatigue and rutting, representing reliable equations for EDF formulation. The impact of overloading was also evaluated, which showed that the increase in pavement deterioration is more than proportional to the increase in axle loads.

6.2 Future Research

On the basis of current research, the following recommendations are proposed for future research:

1. A variety of environmental conditions should be modeled in order to fully represent the wide-ranging environmental conditions that occur throughout Texas. The modeling should include pavements in more locations in order to better evaluate the impact of different environmental conditions on pavement life.
2. Design Guide 2002 includes a feature whereby various climactic conditions can be selected instead of selecting a particular city listed in the software. By virtue of this feature, uncommon locations can be modeled.
3. Another area that merits additional study is evaluating pavements for other distresses such as roughness, thermal cracking, and rutting of individual layers. This work could be possible with future versions of the Design Guide.
4. Currently, Design Guide 2002 has the capability of inputting a maximum AADTT value of 25,000, below which certain structures do not reach failure. In order to overcome this problem, Design Guide 2002 should be upgraded to allow the input of higher AADTT values.
5. In the current research, material selection was based on the 1962 AASHO Road Test. Therefore, another area for further exploration is the analysis of pavement materials typically used in Texas.
6. Additional SNs should be analyzed in order to evaluate a broader range of pavements. This analysis can be done by choosing different thicknesses of various pavement layers, therefore covering a diverse range of structures.

REFERENCES

- AASHO (1962) "The AASHO Road Test" Report 5, Pavement Research, Highway Research Board, Special Report 61E, Publication No. 954, National Academy of Sciences-National Research Council, Washington, D.C.
- AASHTO (1993) *Guide for Design of Pavement Structures*. American Association of State Highway and Transportation Official, Washington, D.C.
- ACVC (2002) "Amarillo Climate" Amarillo Convention and Visitors Council. Accessed from: <http://www.visitamarillotx.com/Climate/>
- Asphalt Institute (1982) Research and Development of the Asphalt Institute's Thickness Design Manual (MS-1), Ninth Edition. Research Report 82-1. College Park, MD.
- Asphalt Institute (1987) "Thickness Design" *Asphalt Pavements for Air Carrier Airports* Manual Series No. 11, Asphalt Institute.
- Ayres, M. and Witeczak, M. W. (1998) "AYMA Mechanistic Probabilistic System to Evaluate Flexible Pavement Performance" Transportation Research Record 1629, Paper No. 98-0738.
- Boussinesq, J. (1885) *Application des Potentials a l'etude de l'equilibre et du Monvement des Solids Elastiques*, Gauthier- Villars, Paris.
- Burmister, D. M. (1943) "The Theory of Stresses and Displacement in Layered Systems and Applications to the Design of Airport Runways" Proceedings of the Highway Research Board, No. 23, Washington, D.C., pp.126-144.
- Croney. D. and Croney. P., (1997) *Design and performance of Road pavements* Mc Graw Hill.
- DUDWMI (2003) "El Paso Climate" Desert USA.com and Digital West Media Inc. Accessed from: http://www.desertusa.com/Cities/tx/tx_elpaso.html
- DRDB (1997) "Rule 425: Use of Cutback Asphalt," Monterey Bay Unified Air Pollution Control District. Accessed from: <http://www.arb.ca.gov/DRDB/MBU/CURHTML/R425.HTM>

- ERES Consultants, Inc. (2002) *Introduction to Mechanistic-Empirical Design of New and Rehabilitated Pavements, Reference Manual* NHI U.S. Department of Transportation, Federal Highway Administration, Course No. 131064.
- GACC (2003) “Austin Climate” The Greater Austin Chamber of Commerce. Accessed from:
http://www.austinchamber.org/Live_Work/Austin_Lifestyle/Climate/
- Groenendijk. J., Vogelzang. C. H., Miradi. A., Molenaar. A. A. A. and Dohman. L. J. M. (1997) “Rutting Development in Linear Tracking Test Pavements to Evaluate Shell Subgrade Strain Criterion” *Pavement Design, Management and Performance Transportation Research Record No. 1570* p.p. 23-29.
- Haas, R. and Hudson, W. R. (1978) *Pavement Management Systems* Mc Graw Hill.
- Harichandran, R. S., Baladi, G. Y. and Yeh, M. (1989) *Development of a Computer Program for Design of Pavement Systems Consisting of Bound and Unbound Materials* Department of Civil and Environmental Engineering, Michigan State University.
- Harman, T. (2001) “Using the Dynamic Modulus Test to Assess the Mix Strength of HMA” US Department of Transportation Federal Highway Association. Accessed from:
<http://www.tfhr.gov/pubrds/mayjun01/dynamicmodulus.html>
- Huang. Y. H. (2004) *Pavement Analysis and Design* Prentice Hall.
- Luskin, D.M. and Walton, C.M. (2001) “Effects of Truck Size and weights on Highway Infrastructure and operations: A Synthesis Report.” TxDOT, CTR, Report- FHWA/TX-0-2122-1.
- Lytton, R.L., et al. (1993) “Development and Validation of Performance Prediction Models and Specifications for Asphalt Binders and Paving Mixes”, Report No. SHRP-A-357, Strategic Highway Research Program, National Research Council Washington, D.C.
- McGhee, K. H. (1999) *Summary of the Proposed 2002 Pavement Design Guide* NCHRP Project 1-37A. Accessed from:
<http://www.2002designguide.com/WSGuideoverview.PDF>

Monismith, C.L. (1992) “Analytically Based Asphalt Pavement Design and Rehabilitation: Theory to Practice, 1962-1992” *Transportation Research Record No. 1354*.

NCHRP (2002) *2002 GUIDE: Using Mechanistic Principles to Improve Pavement Design* NCHRP Project 1-37A Accessed from:
<http://www.2002designguide.com/>

OHPI (2003) *Measuring Pavement Roughness* Office of Highway Policy Information US Department of Transportation Federal Highway Association. Accessed from:
<http://www.fhwa.dot.gov/ohim/hpmsmanl/appe.htm>

Prozzi, J. A. and M. de Beer (1997) “Mechanistic Determination of Equivalent Damage Factors” Proceedings, Eight International Conference on Structural Design of Asphalt Pavements, University of Washington, Seattle.

TxDOT (2004) *Permissible Weight Table* Texas Department of Transportation. Accessed from:
<http://www.dot.state.tx.us/MCD/onestop/permissi.htm>

WSDOT (1998) “Pavement Guide” Accessed from:
http://hotmix.ce.washington.edu/wsdot_web/Modules/09_pavement_evaluation/09-2_body.htm

Yahoo! Inc. (2003a) “Dallas Climate” Accessed from:
http://travel.yahoo.com/p-travelguide-519412-dallas_climate-i

Yahoo! Inc. (2003b) “Houston Climate” Accessed from:
http://travel.yahoo.com/p-travelguide-519419-houston_climate-i

Appendix A
Beta Version of the 2002 Design Guide

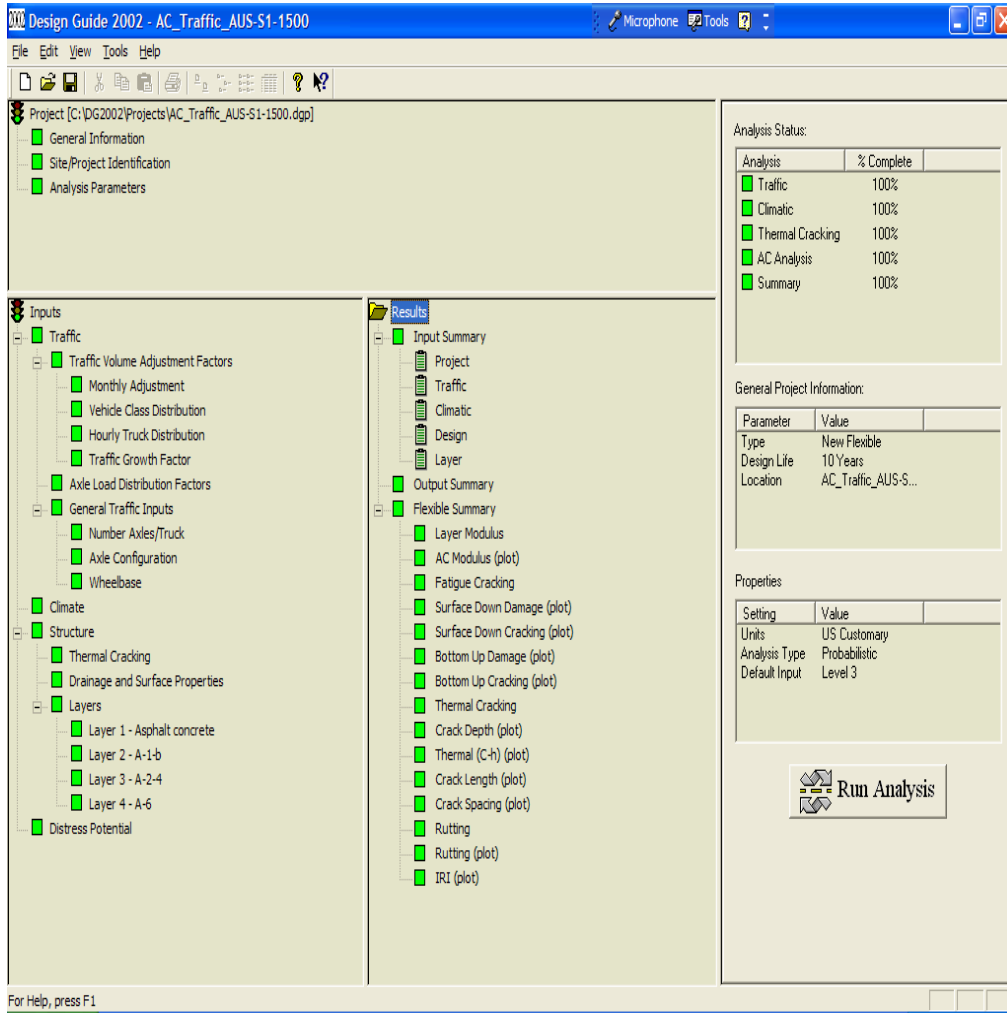


Figure A.1: Input Screen of 2002 Design Guide

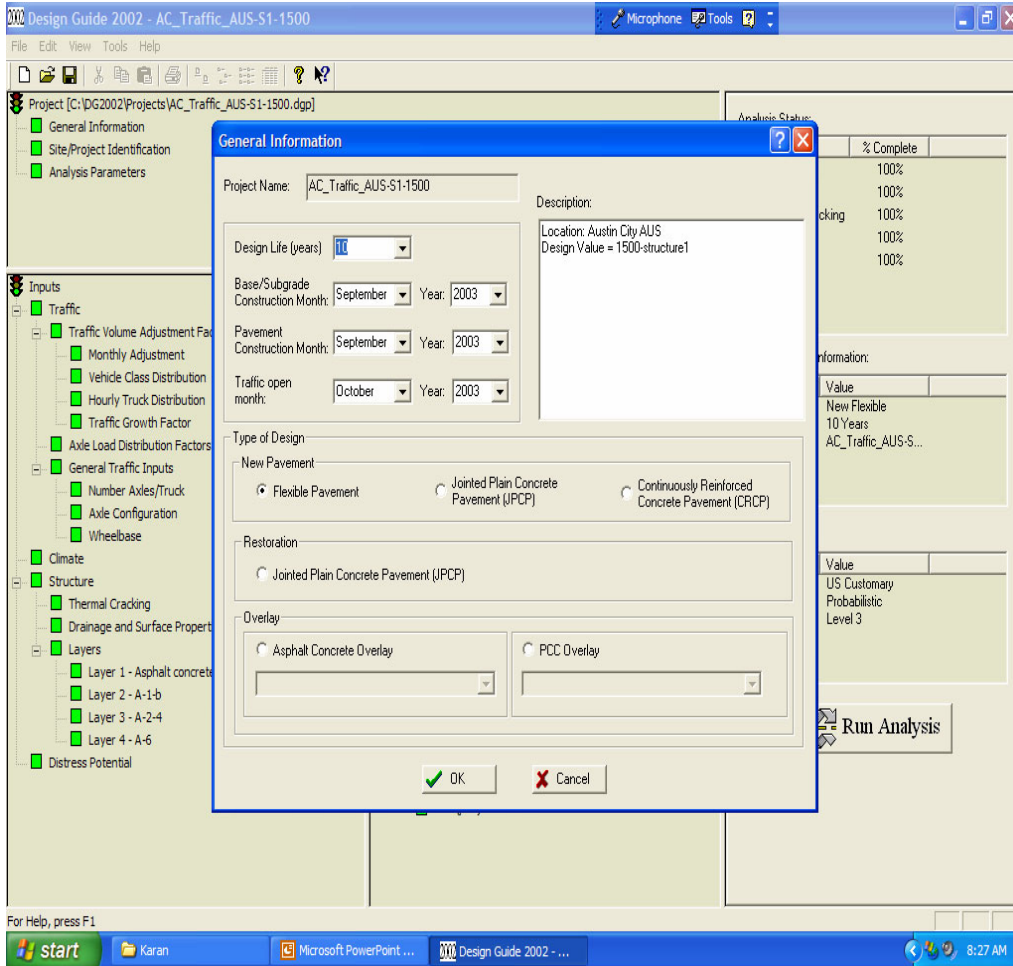


Figure A.2: General Information Inputs

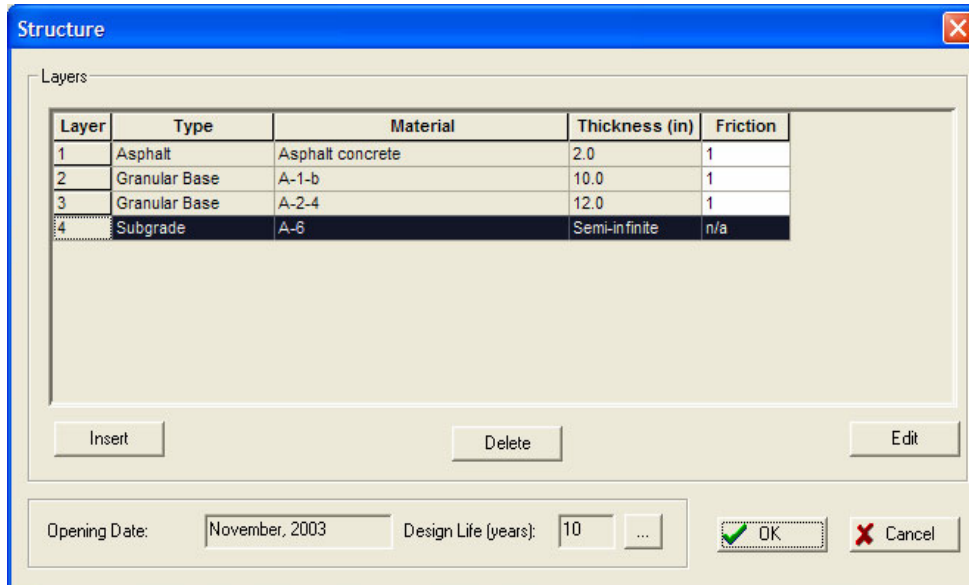


Figure A.3: Pavement Layers

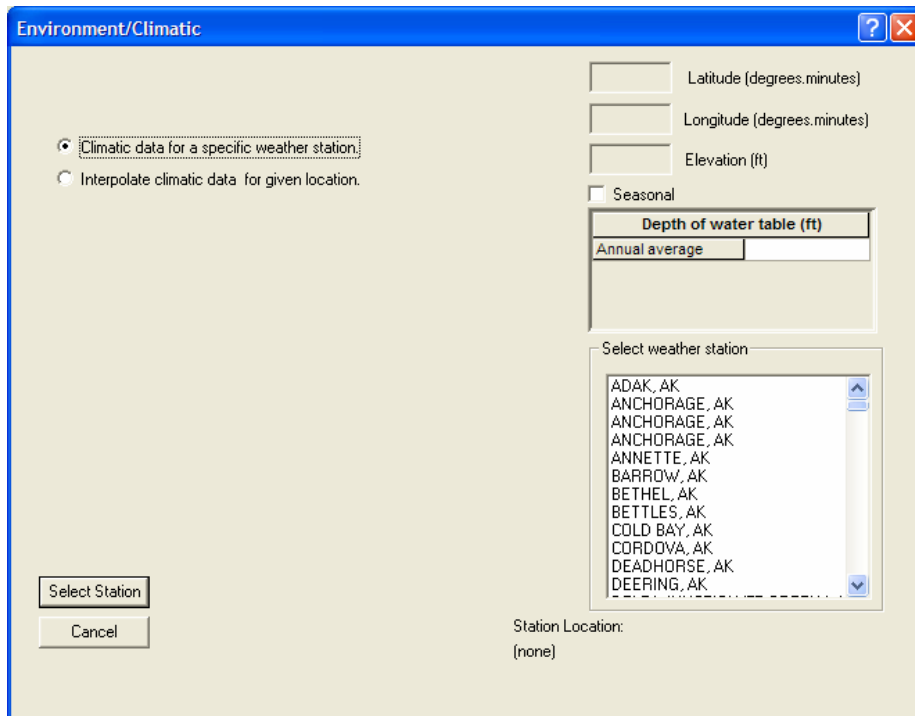


Figure A.4: Locations